Decadal variability of hydrography in the upper northern North Atlantic in 1948-1990

Gilles Reverdin, D. Cayan, Y. Kushnir

JOURNAL OF GEOPHYSICAL RESEARCH, VOL. 102, NO. C4, PAGES 8505–8531, APRIL 15, 1997

Decadal variability of hydrography in the upper northern North Atlantic in 1948-1990

G. Reverdin[1]

Lamont-Doherty Earth Observatory, Columbia University, Palisades, New York

D. Cayan

Scripps Institution of Oceanography, La Jolla, California

Y. Kushnir

Lamont-Doherty Earth Observatory, Columbia University, Palisades, New York

Abstract. We investigate the variability of the North Atlantic subarctic gyre in recent decades from time series of station temperature and salinity. Decadal variability stronger at the surface is identified, which exhibits vertical coherence over a layer deeper than the late winter mixed layer. In the northwestern Atlantic, it corresponds to the layer with a component of water from the Arctic Ocean or from the Canadian Arctic. The spatial coherence of the signal is investigated. An empirical orthogonal function decomposition of lagged time series indicates that a single pattern explains 70% of the variance in upper ocean salt content, corresponding to a propagating signal from the west to the northeast in the subarctic gyre. The most likely interpretation is that the salinity signal originates in the slope currents of the Labrador Sea and is diffused/advected eastward of the Grand Banks over the near western Atlantic. In the northwestern Atlantic, temperature fluctuations are strongly correlated to salinity fluctuations and are aligned along the average *T-S* characteristics. This signal suggests large variations in the outflow of fresh, cold water in the slope current, and is strongly correlated with ice cover. A basin scale atmospheric circulation of weakened westerlies at 55°N, weaker northwesterlies west of Greenland and weaker southerlies over the central and eastern North Atlantic is associated with the high salinity and warm water phase of the first principal component. This circulation pattern leads fluctuations in the northeast Atlantic and lags those in the northwestern part of the basin. The wind indices also suggest that the fluctuations of the fresh water outflow occur during intervals of anomalously northerly winds, either east of Greenland (1965, 1968-1969) or off the Canadian Archipelago (1983-1984).

1. Introduction

Surface marine reports have often served as the basis for numerous studies on the association between low-frequency variations of sea surface temperature and the atmospheric circulation. In particular, near-decadal wintertime variability was identified by *Deser and Blackmon* [1993] (hereafter referred to as DB) as an important mode in the North Atlantic. In that study, which did not include areas in the Labrador and Irminger Seas, a decadal sea surface temperature signal, strongest east of Newfoundland, was found to be related to an atmospheric anomaly pattern in the form of a north-south sea level pressure dipole [see also *Palmer and Sun*, 1985; *Wallace et al.*, 1990]. This configuration corresponds to stronger westerlies over the colder than normal surface waters, an association suggesting that the atmosphere forces a local oceanic response, similar to what is observed on seasonal timescales [*Cayan*, 1992a]. However, DB also point out that the sea surface temperature (SST) signal lags the ice signal in Davis Strait. This suggests that advection by the Labrador Current may be involved in driving the variability east of Newfoundland.

Kushnir [1994] discusses multidecadal variability of temperature and atmospheric circulation in the North Atlantic from a century of gridded Comprehensive Ocean-Atmosphere Data Set (COADS) data [*Woodruff et al.*, 1987]. His study focuses on the ocean surface warming in 1925-1940 and the cooling in 1960-1975. The corresponding SST tendency is of one polarity north of 30∞N, except for some shelf and slope areas off North America where the tendency is opposite. The corresponding atmospheric circulation signal displays some seasonal dependence, with the winter pattern better defined than the summer pattern. The wind deviation from climatology during the warm period (1950-1964) and that during the cold period (1970-1984) have opposite signs: SST warming being associated with both a southward displacement of the belt of westerlies and a cyclonic wind anomaly centered at 45°N. This association is strikingly different from the one found for high-frequency seasonal fluctuations, leading *Kushnir* [1994] to suggest that the atmosphere is not locally forcing the ocean signal but that ocean

[1] Now at Groupe de Recherche de Géodésie Spatiale, UMR CNES/CNRS 5566, Toulouse, France

Paper number 96JC03943.
0148-0227/97/96JC-03943$09.00

advection over the 30°-50°N belt plays an important role in determining the SST anomaly. He also hypothesized that the atmosphere responded to the ocean temperature change.

Salinity signals of several years duration have been found near the sea surface and propagate over large distances in the North Atlantic [*Taylor and Stephens*, 1980; *Dickson et al.*, 1988; *Walsh and Chapman*, 1990]. *Dickson et al.* [1988] identified a low-salinity anomaly, originating in the Arctic or Nordic Seas, which was carried into the slope currents around Greenland and Labrador. It passed east of Newfoundland in about 1974 and was later observed over large portions of the North Atlantic. They proposed that a large low-salinity anomaly could shut off convection in the cold northern seas, where salinity controls surface density, and that the resulting change in vertical mixing would affect winter surface temperature. North of Iceland, there is indirect evidence of such a process in the mid-to-late 1960s, when the vertical stratification associated with the drop of surface salinity induced enough winter surface cooling to cause local ice formation [*Malmberg*, 1969; *Aagaard and Carmack*, 1989]. The timing of the large positive Greenland Sea sea ice anomalies in the mid-1960s and in the northern Labrador Sea and Davis Strait in the early 1970s and mid-1980s also coincided with fresh episodes [*Marsden et al.*, 1991].

One of the low-temperature periods for the northwest Atlantic of DB corresponds to the low-salinity event (the Great Salinity Anomaly, hereafter referred to as GSA) studied by *Dickson et al.* [1988]. Temperature signals associated with the salinity signals have also been identified in some parts of the subarctic gyre [*Taylor and Stephens*, 1980; *Hansen and Bezdek*, 1996], which suggests a direct role of ocean dynamics in the SST fields and therefore in forcing climate variability. The warming in the 1920s described by *Kushnir* [1994] coincided with an increase in surface salinity over large areas of the subarctic gyre [*Smed*, 1943] and was also found in hydrographic time series north of Norway. This change in the distribution of the water masses could be caused by changes in ocean circulation.

The subarctic North Atlantic and Nordic Seas host regions of active exchange (by convection) between the surface layers and the deep ocean. *Dickson et al* [1996] suggest that these exchanges are modulated by the atmospheric circulation. A period of strong northerlies is more favorable for convective mixing. This is related to the North Atlantic oscillation (NAO); hence the northerly wind components east and west of Greenland are out of phase. The latter explains why indices of convective mixing have been in phase opposition in recent decades between the Labrador Sea and the Greenland Sea [*Dickson et al.*, 1996].

The role ocean dynamics have played in the variability of North Atlantic climate in recent decades is not clearly identified because the oceanographic observations are incomplete and most of the previous studies are either based on one particular period or ignore salinity. We attempt here to extend the analysis of the variability of sea surface temperature and atmospheric circulation to the upper ocean temperature and salinity in the subarctic North Atlantic. In particular we are trying to characterize the horizontal and vertical structure of the upper ocean signals, to determine whether or not the coincidence of temperature and salinity fluctuations found during the GSA is normal, and to determine how the water masses are evolving. The discussion focuses on whether or not the salinity signal results from ocean dynamics and in particular from horizontal advection. Time series of sea ice cover and atmospheric winds contribute important additional information to the discussion. The present study is limited by the sparse data coverage; thus the variability of the large-scale circulation, both horizontal and vertical, is not directly resolved.

2. The Data

To address the questions raised in the introduction, we really require gridded fields of temperature (T) and salinity (S) profiles sampled at regular intervals (at least annual), over several decades. Unfortunately, the data sampling is generally sparse in the North Atlantic over decadal time periods, especially outside shelf regions. The exception is for those time periods mapped and studied by *Levitus* [1989a, b]. Thus we base our investigation on a few time series from oceanographic sections or ocean weather ships (OWS) (see Table 1). Most of these time series cover the period of the late 1940s to the late 1980s. This approach was previously adopted by *Taylor and Stephens* [1980] and by *Taylor* [1983], who investigated 24 years of surface temperature and salinity from OWS.

At each site, time series are constructed by first interpolating the individual profiles to a set of fixed depths and then at each depth, binning the data in time. In the rare cases when there are no large gaps in the time series, the average seasonal cycle is estimated by compositing the time series of individual years. In the other cases, the average seasonal cycle is obtained by least squares fit to the intra-annual variability (the shape of the seasonal cycle is prescribed when the time series is too noisy). The average salinity seasonal cycle is rarely significant below 100 m, where its amplitude is usually small compared to the interannual variability. The average seasonal cycle is removed from the binned data to create the deviations. The binned deviations of the best sampled time series are analyzed in the Appendix. These data suggest a red spectrum, so that, even if the time series were poorly sampled, time averaging would filter out the high frequencies while retaining most of the interannual variability. This is done here by averaging the deviations from the seasonal cycle over a year or a particular season. These deviations are fitted by a cubic spline to create a time series which is then smoothed by a running average (weights 0.25, 0.5, and 0.25 for successive yearly values).

Errors in the reconstructed anomalies result from insufficient sampling of the subseasonal variability, uncertainties in the derived seasonal cycle, and spatial inhomogeneity (in those places where spatially separated data were grouped in a single time series). Even for the best time series, there are periods of a few years with no data. These data gaps were filled by temporal interpolation or by using ancillary data not collected at the same site. Fortunately, although the gaps are more common before 1954 and in the late 1980s, they do not happen at the same time for different sites so that some spatial averaging might help. Also, data errors are more common before 1954 and so reduce the accuracy of the earlier part of the record at many sites. Examples of time series and a discussion of the effect of sampling on the accuracy of the reconstructed time series are presented in the Appendix.

Not all the OWS were regularly collecting vertical profiles of salinity. Because we need to assess the vertical structure of the interannual variability, we only incorporate the subset of sites for which some vertical sampling (bottle or conductivity-temperature-depth (CTD) casts) was obtained. The following stations are included: OWS Mike (66°N, 2°E) between 1948 and 1992 [*Gammelsrød and Holm*, 1984; *Gammelsrød et al.*, 1992]; OWS India (59°N, 19°W) between 1958 and 1976 and OWS Lima (57°N, 20°30'W) between 1976 and 1990 (these two are merged in a single time series); OWS Bravo (57°N, 45°W) in the southern Labrador Sea, which has regular sampling between 1964 and 1974 [*Lazier*, 1980] and a looser sampling from 1948 to 1995 [*Lazier*, 1995]; OWS Charlie (52°45'N, 35°30'W) between 1958

Table 1. Location of the Principal Time Series and Characteristics of the Sampling

Site Name	Position	Period Sampled	Comments
Fylla Bank	64°N, 54°W	1948-1988	only April-October
OWS Bravo	57°N, 45°W	1948-1995	regular sampling only for 1964-1974; after 1988, radiomessages
Hamilton slope	54°50'N, 53°30'W	1948-1995	only May-September; after 1988, radiomessages
Flemish Cap	47°N, 47°W	1948-1995	after 1988, radiomessages
Grand Banks slope	43°N, 49°W	1948-1988	
OWS Charlie	52°45'N, 35°30'W	1948-1990	regular sampling only for 1958-1990
OWS Alpha	62°N, 33°W	1948-1991	regular sampling only for 1954-1974
Irminger Sea	64°30'N, 28°W	1948-1990	irregular sampling
SI (Selvogsbanki)	63°N, 22°W	1948-1992	irregular sampling before 1971
OWS India-Lima	59°N, 19°W 57°N, 20°30'W	1948-1975 1975-1990	includes also data at 60°N, 20°W
Rockall Channel	56°N, 11°W	1948-1992	surface sampling [*Ellett*, 1982]
Faeroe-Shetland Channel	61°-61.7°N, 3°-4°W	1948-1992	
OWS Mike	66°N, 2°E	1948-1992	
Bear Island section	74°N, 20°E	1950-1992	from *Loeng et al.* [1992]
Station S	32°12'N, 64°30'W	1948-1992	

and *1990 [Levitus et al.*, 1995], which we extended back to 1948 using a few additional stations. We construct a time series for the central Irminger Sea by combining station data in 1954-1974 from OWS Alpha with a few neighboring station data and more numerous temperature profiles.

Other time series are constructed along sections sampled seasonally or less frequently and designed to survey particular currents or water masses, often close to shelves. Some of these time series were used by *Dickson et al.* [1988] to investigate the propagation of the GSA from the mid-1960s to the late 1970s. We also construct time series from sections sampled seasonally in the central and eastern Icelandic Sea [*Malmberg*, 1969, 1984; S.-A. Malmberg et al., Long time series in Icelandic waters, unpublished manuscript, 1994], off the Selvogsbanki south of Iceland, and in the Irminger Sea west of Iceland [*Malmberg and Kristmannsson*, 1992]. The published monthly averages of surface temperature and salinity from the Rockall Channel west of Scotland [*Ellett*, 1982; *Ellett and McDougall*, 1983; D.J. Ellett and W.R. Turrell, Increased salinity levels in the NE Atlantic, unpublished manuscript, 1992] are included up to 1992, as well as time series north of Norway, near 74°N, 20°E [*Dickson and Blindheim*, 1984; *Blindheim and Loeng*, 1981; *Loeng et al.*, 1992]. We also construct a 1948-1992 time series in the central Faroe-Shetland Channel 61°-61.7°N, 3°-4°W (stations 6-7 of the Nolso-Flugga section) [*Dooley et al.*, 1984; D.J. Ellett and W.R. Turrell, Increased salinity levels in the NE Atlantic, unpublished manuscript, 1992].

The smoothed maps of temperature and salinity in the northern North Atlantic (Figure 1) show that most of the sites in the interior are within regions of relatively weak gradients, in the domain of the subpolar mode water for which T and S decrease from south to north and from east to west. Charlie is north of the Subarctic Front where water is relatively fresh, since it contains water of Polar or Arctic origin, flowing from the slope current off Newfoundland. In the eastern portion of the subarctic gyre, there is a larger contribution from the salty subtropical water of the North Atlantic Current. The hydrostation S (also referred to as "Panulirus") off Bermuda at 32°12'N, 64°30'W provides the only upstream time series in subtropical water, although it is not known to what degree these data are representative of the water flowing further north in the North Atlantic Current. *Joyce and Robbins* [1996] present a more recent time series at this site than used in earlier studies, including *Frankignoul* [1981], *Talley and Raymer* [1982], and *Jenkins* [1982].

For the sites in the slope current which flows cyclonically around the Labrador Sea and along the Grand Banks, horizontal gradients in the upper layer are very large on scales of 50 km. Around the Labrador Sea, narrow baroclinic currents are centered on the upper part of the slope with freshest and coldest water near the surface and onshore [*Lazier*, 1982]. The near-surface water originates from the Arctic with an onshore component partially derived from the Baffin Bay and Hudson Bay waters [*Myers et al.*, 1990; *Mertz et al.*, 1993], whereas the warmer and saltier water found offshore and at the subsurface partially originates from the Irminger Sea. The hydrographic variability at different distances from the shelf can have different components. However, the analysis of the T-S variability across the Flemish Pass presented in section 3 suggests that a large part of the variability can be interpreted as vertical displacements of isopycnals, which are less dependant on the distance from the shelf than is the water composition. Therefore one site centered in the slope current region should be representative of the average salinity and temperature transported by the current. For the Labrador Current at 55°N, the current core is located close to the 500- to 800-m isobaths [*Lazier and Wright*, 1993]. At other slope sites, our choice is somewhat constrained by the sampling, but we

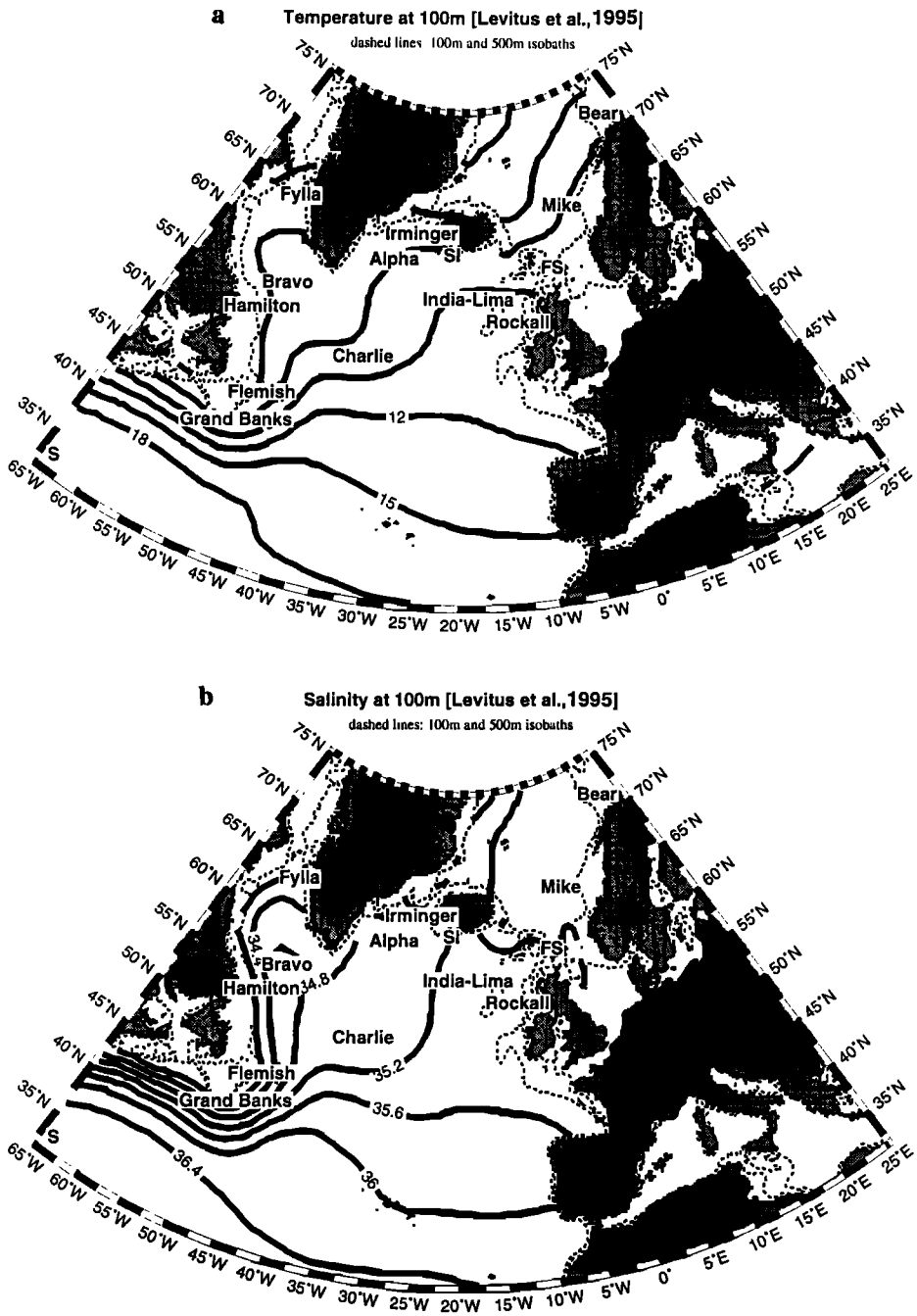

Figure 1. (a) Climatological temperature in degrees Celsius and (b) salinity at 100 m from the *Levitus et al.* [1995] climatology. Positions of the main time series are indicated with their names (S for ocean hydrostation S (also referred to as Panulirus), FS for "Faroe-Shetland," SI for "South Iceland"). The 100- and 500-m isobaths are also drawn on all maps.

only retain sites where the ocean depth is between 300 and 1500 m. This includes time series taken off the Fylla Bank west of Greenland near 64°N [*Blindheim*, 1974; E. Buch and M. Stein, Temperature and salinity at the Fylla Bank section, West Greenland, unpublished manuscript, 1987], from the Seal Island section near 55°N east of Hamilton Bank, west of Labrador (R.A. Clarke, Changes in the western North Atlantic during the decade beginning in 1965, unpublished manuscript, 1984), along 47°N west and east of the Flemish Cap [*Keeley*, 1982], and further southeast east of the Grand Banks.

3. Vertical Structure of Low-Frequency Variability

Low-frequency time series of T and S are presented for a few sites in the western subarctic gyre (Figure 2). At each site, the curves correspond to different depths, starting with a depth close to the base of the winter mixed layer (each curve is referenced to its climatological value for March-April, which is the time of deepest penetration of convective mixing). These time series display quasi-decadal variability well below the base of the

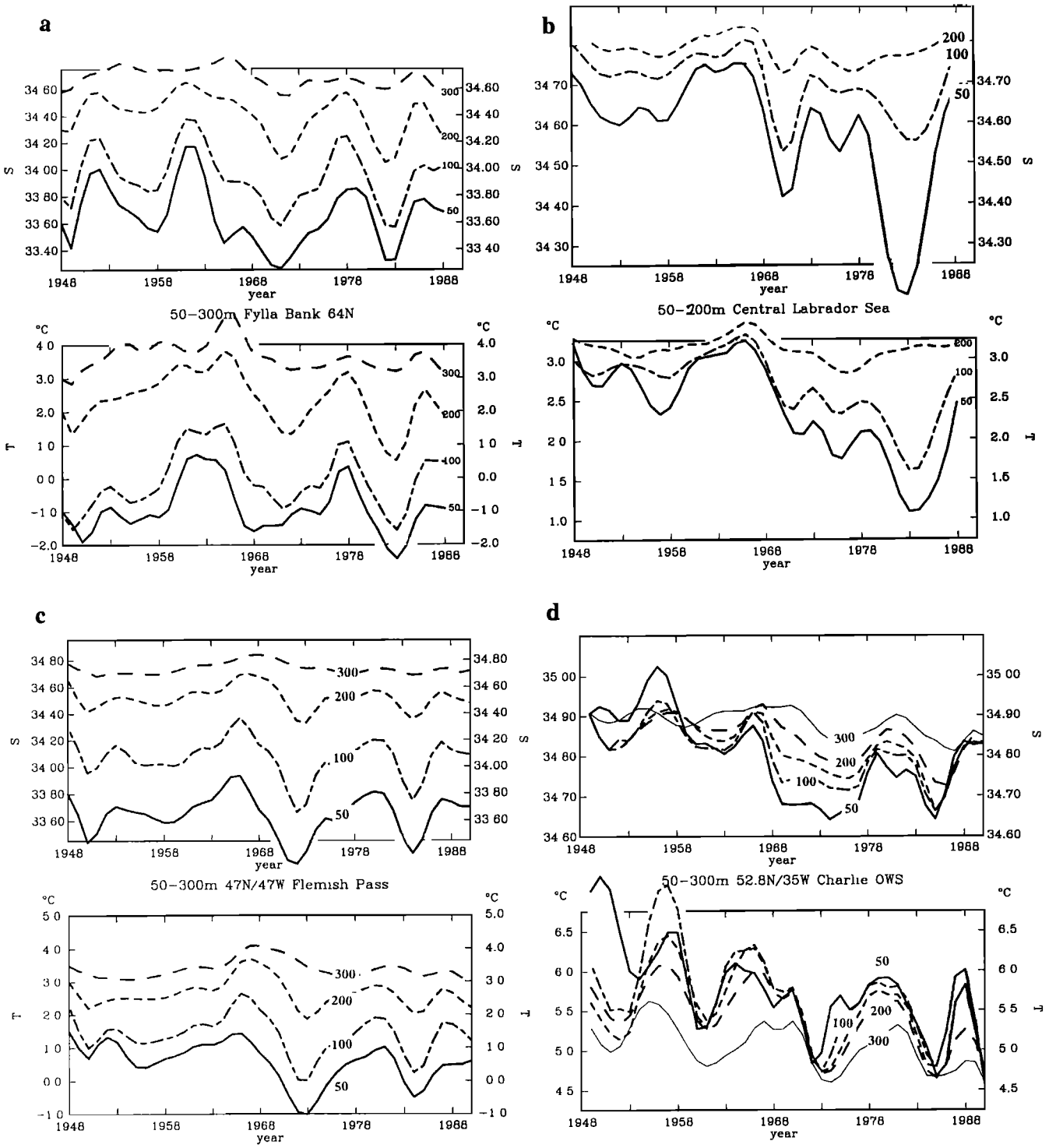

Figure 2. Low-passed time series of temperature and salinity after removal of the seasonal cycle and smoothing by a 1-2-1 filter over successive years (the average for the season March-April is added at each depth). For the selected sites, time series at different depths are plotted (the corresponding depths are indicated near the right side of the Figure). Few data at Bravo in 1975-1988, and at Charlie in 1948-1958 result in larger uncertainties for those periods.

winter mixed layer. The curves also suggest that the signal decreases with depth. An analysis of lagged correlation is done to quantify the similarities between the signal at different depths. The most prominent salinity signal near the surface is indeed correlated vertically with the signal within the stratified layer. On the basis of the temporal correlation of the signal, we conservatively estimate that a correlation coefficient of 0.7 is statistically nonzero at the 95% level. In the slope current around the Labrador Sea, the level where the correlation drops below 0.7 is near the base of the strongly stratified upper ocean which contains a component of cold and fresh water of Arctic origin. At Mike, the drop of correlation takes place within the thermocline

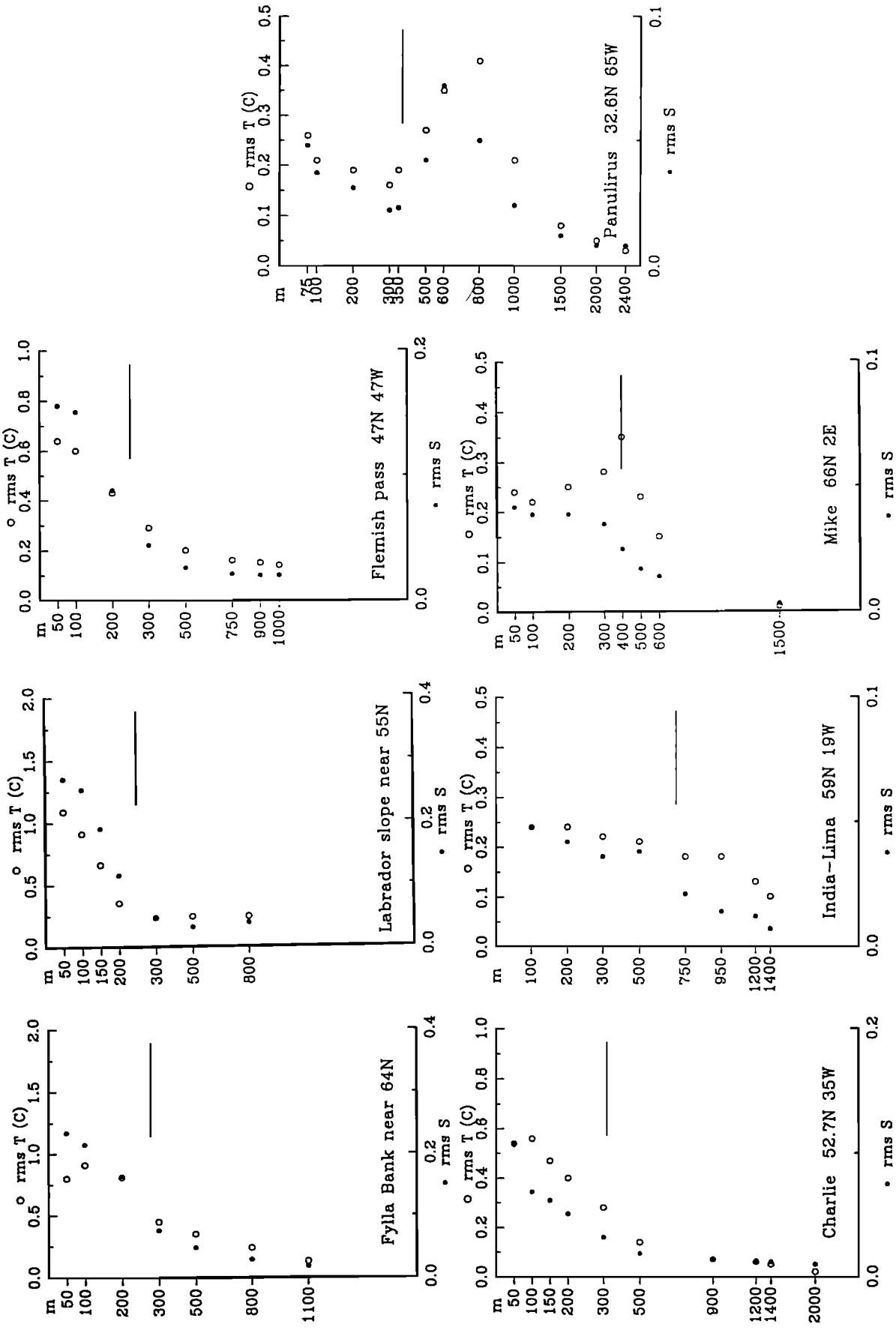

Figure 3. Root mean square interannual variability of T and S at a few sites as a function of depth. Open dots are for temperature and solid dots are for salinity (the ratio of the scales is always 1°C/0.2). The horizontal bars indicate the level where the correlation coefficient of salinity with the upper ocean salinity drops below 0.7.

near 400 m in the transition layer between the warm and salty surface water and the colder and fresher intermediate waters from the northern European Seas. At S, the decorrelation occurs below the less stratified layer of 18°C which includes water of subtropical origin. In the northeast Atlantic and the eastern part of the subarctic gyre, the winter mixed layer is usually deeper than in the western subarctic gyre. The similarity between the variability in the winter mixed layer and below is also found at the other sites, in particular for salinity, to at least 100 m deeper than the average base of the winter mixed layer.

The depth dependency of rms variability of T and S is presented for typical sites in Figure 3. The horizontal bar indicates the level for which the correlation with the surface drops below the 95% significance level. At most sites, the rms low-frequency variability decreases monotonically with depth, both for T and S. At some of the deepest levels where correlation is significant, there is a suggestion that the variability lags the surface one. Among the examples presented earlier in Figure 2, this appears most clearly for salinity at 300 m for the Fylla Bank site and at 200 m for the Flemish Pass site. This is also very noticeable for salinity at 400 m at OWS Mike and in the central Faroe-Shetland Channel (which both show a 1-year lag with respect to the mixed layer time series in the upper 200 m). At station S, salinity at 300-350 m in what is usually the 18°C water thermostat presents a 1-year lag compared to the upper 100-m mixed layer time series. The 1-year delay at this last site roughly corresponds to the ventilation age of this thermostad water, found a year earlier near the surface, presumably further to the northeast [*Talley and Raymer*, 1982; *Jenkins*, 1982; *Jenkins and Goldman*, 1985]. We found no evidence of a significant lagged correlation between the surface and deeper levels, although in the central Labrador Sea and at Flemish Pass, the quasi-decadal component of the variability in salinity below 300 m seems to be anticorrelated with the surface signal. However, because lower frequencies are present which do not change sign between the surface and these depths, the overall correlation coefficient is not significantly different from zero.

At OWS Mike, the large temperature variability near 400 m corresponds to a layer of increased temperature stratification. Inspection of the T-S diagram indicates that at 400 m, any vertical displacements resulting in observed rms temperature variability of 0.35°C would be associated with a rms salinity variability of 0.014, which is less than observed. The salinity variability at this depth is quite similar to that on isopycnal surfaces near this depth (for instance σ=27.9). Both are correlated at a lag of 1 year with the salinity variability in the mixed layer (with a correlation coefficient of 0.95). However, the temperature at this depth and the vertical displacements of the isopycnals are not correlated with the surface layer variability. This difference between the isopycnal changes of water mass characteristics and the thermocline displacements results in a lack of correlation between temperature and salinity changes at 400 m.

At station S, there is an increase in both temperature and salinity variability below 350 m. These variables are highly correlated (correlation of 0.9, in contrast to 0.2 in the upper 350 m). The variability in T-S space is mostly aligned along the mean T-S characteristic [*Levitus*, 1989a; *Joyce and Robbins*, 1996; *Houghton*, 1996]. This means that at fixed depth in the thermocline, any change in T and S due to the vertical displacements will be larger than changes in the T-S relationship due to variability in the thermocline ventilation [*Jenkins*, 1982; *Talley and Raymer*, 1982; L.D. Talley, North Atlantic circulation and variability, Submitted to the conference on Nonlinear Stability, 1996].

At these sites, OWS Mike and station S, the vertical displacements of the thermocline (halocline) are not well correlated with the near-surface variability. The situation is very different at the western North Atlantic slope current sites on the rim of the Labrador Sea. There, although the upper ocean is strongly stratified, isopycnal displacements are correlated with the near-surface salinity and temperature variability (taken at 50 m, near the base of the late winter mixed layer). In contrast, salinity changes on isopycnal surfaces are not well correlated with isopycnal displacements. This is seen at 47°N, 47°W for the isopycnal surface σ=27.4 (Figure 4). For this example, salinity changes on the isopycnal surface are less than salinity changes at fixed depth and are not correlated with near surface changes (at 50 m).

Analyzing the variability in the T-S relationship helps identify the mechanisms responsible for the salinity variability. The T-S diagram is plotted for each year at selected depths. For the two northern sites (Figures 5a and 5b), the T-S relationships for individual years overlay each other and are aligned along the average T-S curve. The surface variability therefore introduces large density changes. Since there is no variability in the subsurface water masses at these sites (and so little salinity variability on selected isopycnal surfaces), we conclude that changes in isopycnal mixing between the Arctic water mass and the more salty offshore component are not responsible for the variability. There is more interannual variability in the T-S curve downstream from the Labrador Sea, at the well-sampled Flemish Pass section at 47°N, 47°W (Figure 6a) and at Ice Patrol survey sites farther south along the Grand Banks [*Petrie and Drinkwater*, 1993], (i.e., changes of T and S on isopycnal surfaces). These fluctuations are such that at a given depth there is less interannual

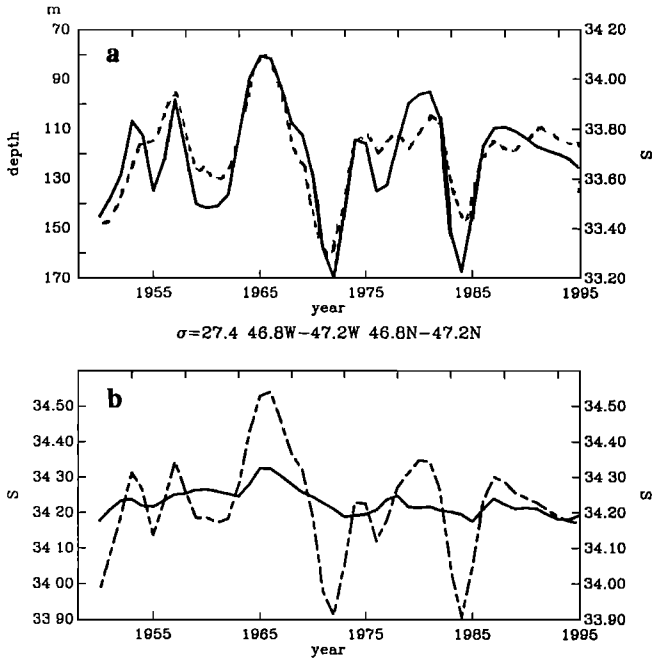

Figure 4. Time series at 47°N, 47°W: (a) solid line for the depth of the σ=27.4 isopycnal surface (centered near 130 m) and dashed line for salinity at 50 m (base of the winter mixed layer); (b) salinity on σ=27.4 (solid line) and salinity at 130 m (dashed line).

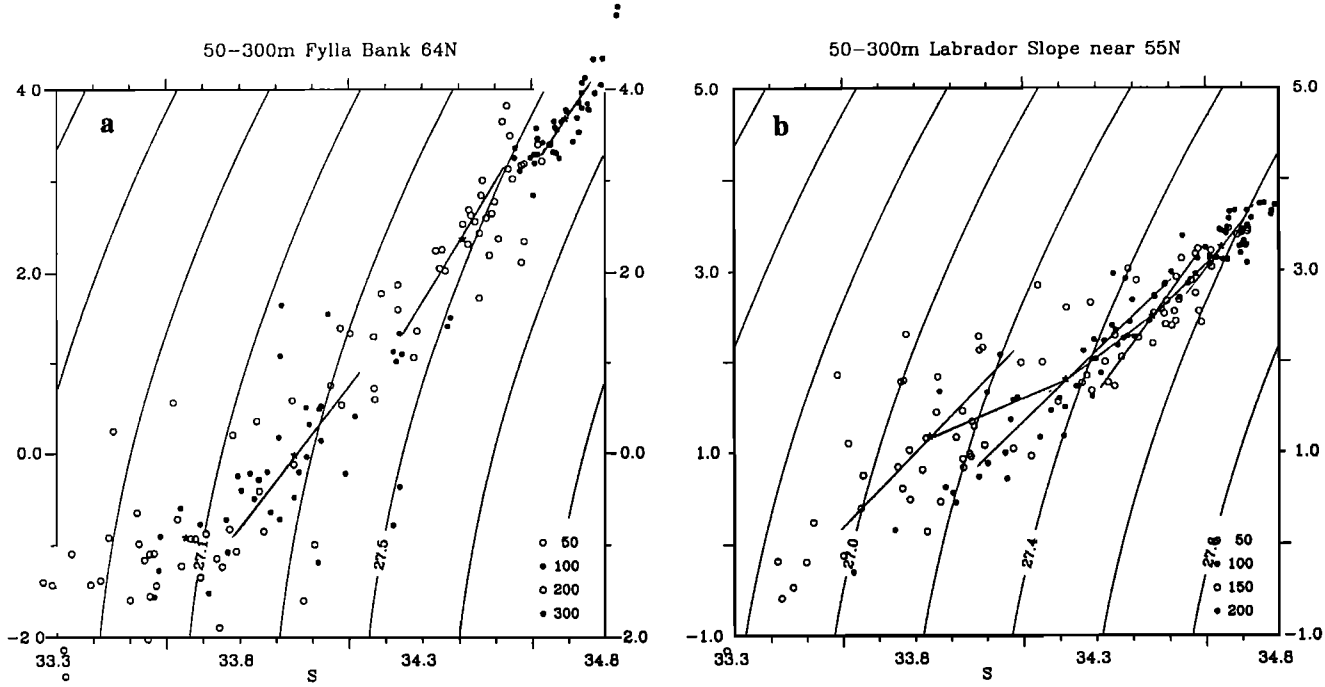

Figure 5. *T-S* diagrams of the low-passed time series sampled once a year for Hamilton and Fylla Bank. For each site, different levels are represented by different symbols. The climatological average *T-S* curve is usually plotted as well as the principal axis of the *T-S* distribution at each depth (the average value at 50 m for the Hamilton Bank (Fylla Bank) sites is more uncertain, because the seasonal cycle is based on data collected mostly between May and October (April and September); there, an error in the average late winter (*T*,*S*) is likely to have resulted in the shift of the *T-S* diagram to a higher *T* than real).

density change than if the variability was along the average *T-S* relationship. The main change in the *T-S* characteristics of the subsurface variability occurs east of the slope (Figure 6b) where the water of the slope current spreads into the interior and is strongly mixed with North Atlantic Current water (see also Figure 6c for Charlie). The average *T-S* curve is shifted toward higher *T* and *S* on isopycnals and has a different slope than in the slope current. In this case, *T-S* variability at each depth level is aligned mostly along isopycnal characteristics, not along the average *T-S* curve. This implies that isopycnal surfaces in the interior experience much less vertical displacements than isohaline surfaces. These isopycnal displacements in the interior are also smaller than in the slope current. We will analyze what these observations imply in the discussion chapter.

In order to estimate the heat and salt content changes related to the surface processes, we vertically integrate temperature and salinity down to the level *H*, where the correlation with the near surface is no longer significant. This can be done because the time series at different levels within the upper ocean are correlated. Vertical integrals are also less noisy than the time series at the individual levels. We set the lower boundary of the averaging at the level where the correlation to the uppermost subsurface level drops below 0.7 and refer to the vertical integrals as depth-integrated temperature and salt content. The average temperature and salinity from 0 m to *H* will be referred as near-surface temperature (*T*) and salinity (*S*). These vertically averaged time series are not very sensitive to the choice of *H* because *H* also corresponds to the level at which rms variability diminishes (particularly for *S*). *H*, which defines a vertical scale for the upper ocean variability, is less than 100 m in the Icelandic Sea, 150 m in the central Labrador Sea, around 200 m in the slope currents around the Labrador Sea and Grand Banks, up to 300 m at Charlie and S, 400 m at Mike, and 500 m or more at the other eastern and northern sites of the subarctic gyre, where the winter mixed layer is deepest. There are two sites, Rockall Channel and the station north of Norway, for which we have times series at only one level (surface and 200 m, respectively). For those, we determine *H* based on a combination of local winter mixed layer depth estimated from station data and from *H* values of nearby sites. *H* is extremely variable across the slope current for the Flemish Pass section, where it varies from 300 to 150 m across the 50-km-wide slope current. At the other sites in the current, such an analysis is not possible. There, a vertical scale representative of this current is estimated by comparison to the Flemish Pass transverse structure of *H*. This amounts to reducing *H* by 20 off the Fylla Bank (200 m) and to 150 m off the Hamilton Bank.

4. Horizontal Structure

4.1. Temperature and Salinity Variance

We want to investigate the spatial structure of the variance in near-surface temperature and salinity, as well as in the vertically integrated temperature and salinity content. The following presentation is based on maps for which values are plotted at the corresponding sites. We assume that the time series are representative of their surroundings so we can interpret the large-scale spatial distribution of properties from the isolated sites (refer to Figure 1 for the near-surface water mass characteristics of the North Atlantic).

The low-frequency rms *T* variability is largest in the western and central subarctic gyre (Figure 7a), as well as close to the shelf

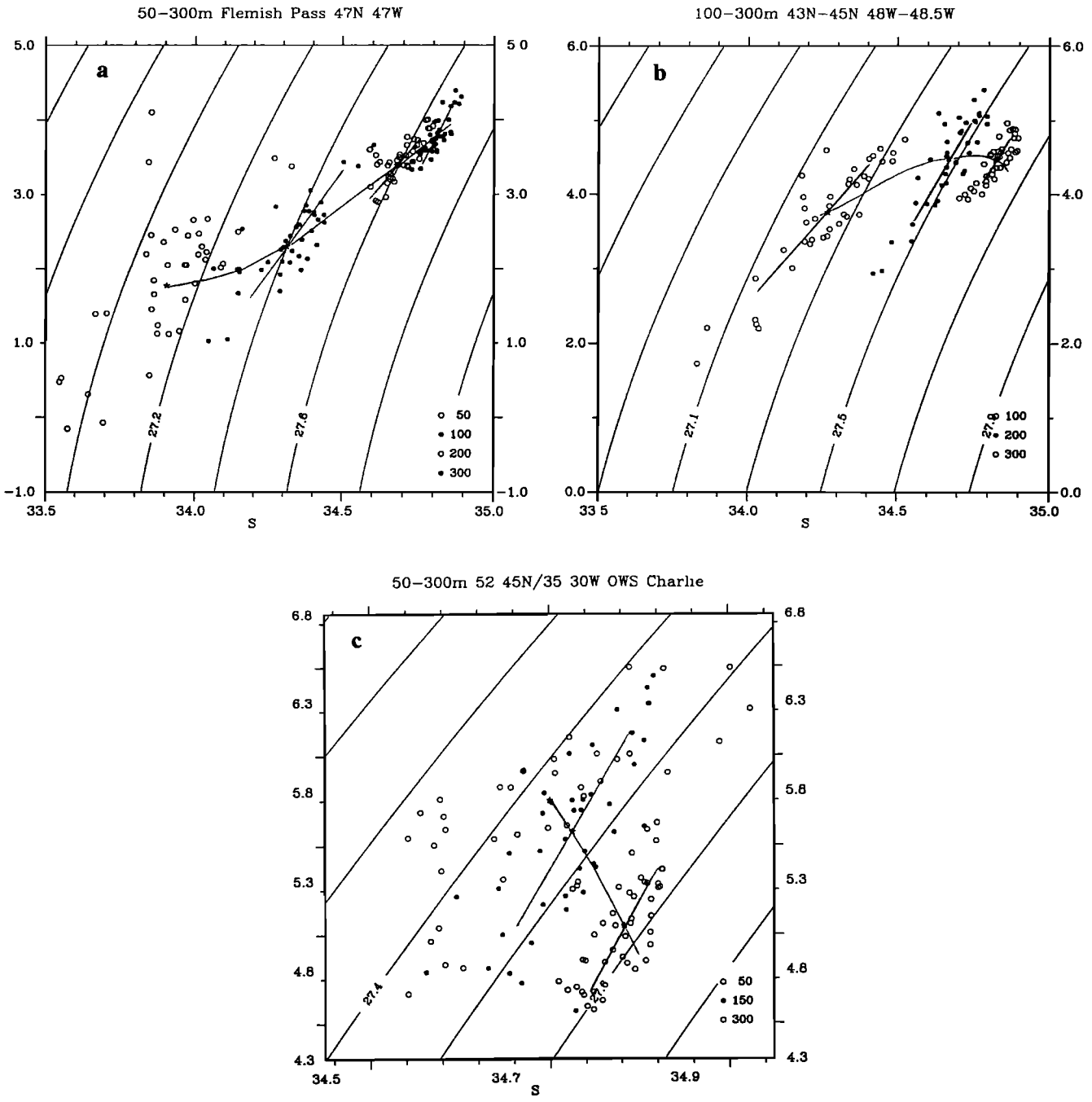

Figure 6. Same as Figure 5, but for other sites of the northwestern Atlantic.

break, north of the Gulf Stream (these latter time series are, however, shorter and will not be included in subsequent analysis). This distribution is also noted in the EOF associated with decadal variability of winter SST of DB. The east-west contrast is even more pronounced for salinity rms variability (Figure 7b), with very high rms values of S located in the slope current around the Labrador Sea and the Grand Banks where it is at least a factor 3 larger than at other open ocean sites.

The low-frequency rms variability of salt content (Figure 7c) is largest in the slope current (order 30 m), compared to 20 m or less elsewhere, including the central Labrador Sea (note that in these calculations, S has no dimension; a change of salt content of 30 m is equivalent to an addition/removal of roughly 0.9 m of fresh water from a water mass with salinity of 34.0, a value typical of the near-surface Labrador Sea). The spatial gradient of the rms variability of salt content is weaker than for S, because the changes in the vertical scale of the upper ocean signal (H) partly compensate for the changes in S rms variability. This is consistent with the spatial variations in S variability found for the GSA by *Dickson et al.* [1988]. The rms heat content variability (not shown) is largest in the central Irminger Sea because the large T signals off Iceland are associated with very large vertical scales.

To estimate the relative importance of salinity and temperature variability on the rms density fluctuation $\sigma\{\rho\}$ and hence on the changes in upper ocean vertical stratification, we examine the

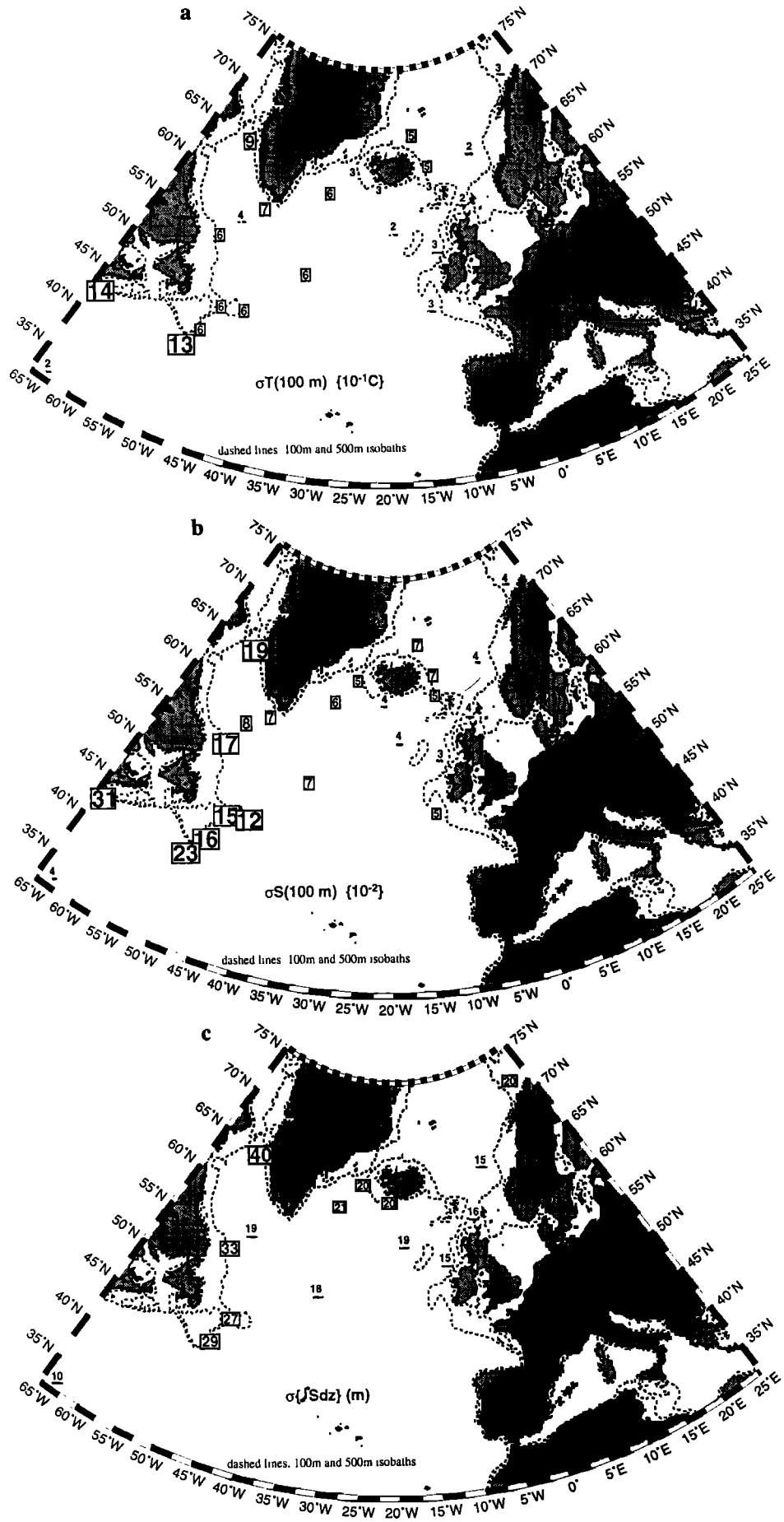

Figure 7. Rms low-frequency variability of (a) temperature at 100 m (degrees Celsius), (b) salinity at 100 m, and (c) salt content (meters). Large values are boxed and the font size increases with its magnitude.

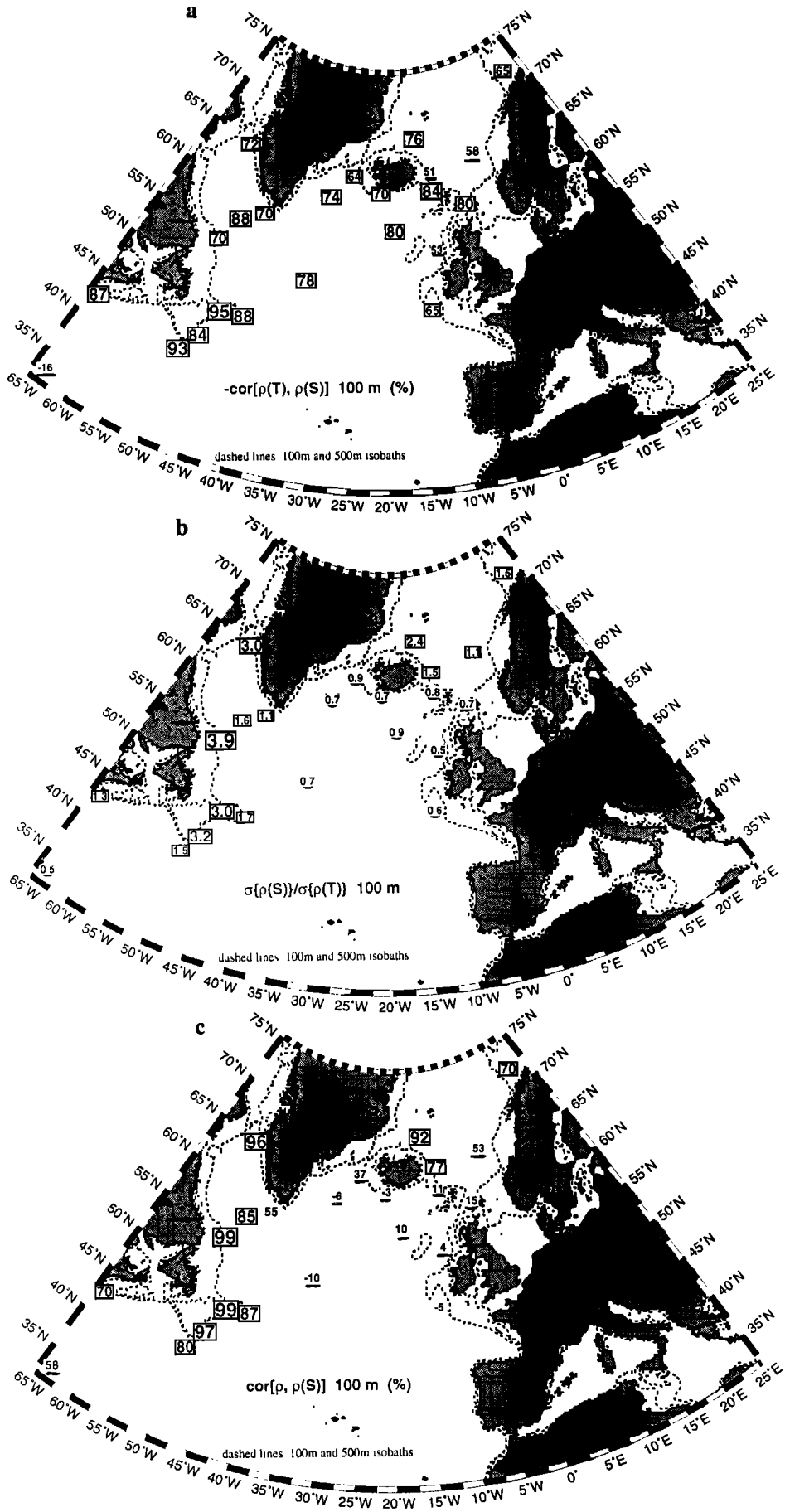

Figure 8. (a) The correlation coefficient between the contributions of temperature and salinity to low-frequency density deviations (minus the correlation between temperature and salinity deviations). (b) The correlation coefficient between density fluctuation and the salinity contribution to its variability. (c) The ratio of the temperature and salinity rms contributions to density variability. Significant correlation coefficients or large values are boxed and the font size increases with its magnitude.

density time series estimated assuming either T or S constant, $\rho(S)$ and $\rho(T)$, respectively, at one level within the upper layer (100 m). Results at other levels or for the vertically integrated quantities are comparable. In Figure 8a we present the correlation between $-\rho(S)$ and $\rho(T)$, which is nearly identical to the correlation between T and S. Figure 8b shows the ratio $\sigma\{\rho(S)\}/\sigma\{\rho(T)\}$ of the rms contributions of salinity and temperature to density variability. Figure 8c shows the correlation between ρ and $\rho(S)$. There are large areas where the correlation between temperature and salinity variability is positive and statistically different from zero (i.e., > 0.7). This is particularly the case for the sites with colder temperatures along the slope off Labrador and the Grand Banks. There, the salinity contribution to density variability dominates that of temperature by more than a factor 3. This is due to the low ratio of T-S variability and also to the small steric changes resulting from temperature changes at a low temperature. The correlation between T and S is often weaker in the northeastern Atlantic. This is probably a real feature, although the higher correlation at the well-sampled site in the central Faroe-Shetland Channel suggests that large uncertainty in the (small) temperature signal at the other sites contributes to the low correlation. The ratio $\sigma\{\rho(S)\}/\sigma\{\rho(T)\}$ presents large regional contrasts (Figure 8b). The contribution $\sigma\{\rho(S)\}$ from salinity dominates that of temperature in the cold water north of Iceland but is smaller in the warmer water south of Iceland. There is no correlation between anomalous temperature and salinity at station S (lower left corner of the plot), where $\sigma\{\rho(T)\}$ dominates $\sigma\{\rho(S)\}$ by almost a factor of 2.

Usually, temperature and salinity have an opposite effect on density variability. Where the contributions of the two are of a near equal magnitude, the correlation between ρ(S) and ρ is small. The value of $\sigma\{\rho\}$ in regions of equal T/S contribution is very small if the correlation between T and S is high, for example, at India-Lima in the northeast Atlantic.

4.2. Spatial Structure of Variability

Time series of T or S at nearby sites are often significantly correlated. This suggests that although the spatial sampling is obviously rudimentary, we can also interpret the spatial structures from the joint analysis of the time series. To analyze the covariance between time series, we perform an empirical orthogonal function (EOF) analysis using the different sites. For salt content (Figure 9a), a large portion of the signal is distributed between two principal components (PCs) which together account for 80% of the total variance. The second PC is correlated with the first one at a level of 0.86 with a lag of 4-5 years. The first EOF explains variance mostly in western stations (Figure 9b), whereas the second EOF explains a higher percentage of the variance in the north and northeast (Figure 9c). The large dip in the early 1970s for the first PC (Figure 9a), followed in the mid 1970s by a dip in the second PC, corresponds to the GSA, for which a propagation signal around the subarctic was first detected [*Dickson et al.*, 1988]. A 4- to 5-year lag is also found for the other peaks and troughs, so that for these oscillations of shorter duration the two PCs (characteristic of east and west stations) are in phase opposition. The lag between the two time series together with the separation in spatial structures suggests a signal propagating from the west to the northeast.

Lag correlations between time series are investigated to characterize further the structure of the variability. The lagged correlations of the salt (heat) content between different sites indicate that nearby sites are better correlated than distant ones, in particular, when they are in a similar water mass. Usually, the maximum correlation is found at lags different than zero. The largest distance over which significant correlation is detected is about 4000 km between Charlie leading the station north of Norway by 3.5 years. The time series which correlate least with the others are the ones north of Iceland and the one in the central Labrador Sea.

To investigate possible propagation of the salinity signal, we estimate the maximum lagged correlation at which the correlation between pairs of nearby stations. We start from OWS Charlie, a central location, and from there move from station to station to cover the entire set of stations and derive a map of the lags with respect to Charlie (Figure 10a). The value indicated for the central Labrador Sea is marginally significant, because correlation with nearby sites is low. The lags with respect to Charlie correspond closely to the ones given by *Dickson et al.* [1988], except for the Fylla Bank series, for which the lag with the Flemish Pass is found to be 1.5 years. There is a hint of a salinity signal propagating in an anticlockwise direction along the rim of the Labrador Sea and then toward the northeastern Atlantic and northern European Seas. The increasing lags in the northeastern Atlantic correspond to the propagation of the low- and high-salinity anomalies from the southwest to the northeast, as illustrated in Figure 10b for sites within the North Atlantic water or modified North Atlantic water. Propagation of salinity variability in that area was already clearly established from a subset of weather ship surface data analyzed by *Taylor and Stephens* [1980]. This is also consistent with the observations of the GSA discussed by *Dickson et al.* [1988] (with a difference in timing between the Fylla Bank area and the Flemish Pass). There is, however, some deformation of the signal, and locally, the reason for time evolution might be different. For instance, the sections around the Faroe Islands (not shown) can exhibit different hydrographic variability, which suggests that locally variability might result from displacements of the fronts and associated currents (B. Hansen and R. Kristiansen, Long-term changes in the Atlantic water flowing past the Faroe Islands, unpublished manuscript, 1994).

The lagged correlation coefficients for temperature are lower than for salinity. There is clear indication of temperature propagation along the continental slope in the northwestern Atlantic. There, the time series off the Grand Banks lag those from the northern Labrador Sea, similarly to what is found for salinity. No temperature propagation is found elsewhere. This differs from the conclusions of *Hansen and Bezdek* [1996], who identify a temperature signal propagating from southwest to northeast in the subarctic gyre.

The observed lag relationship between salinity time series at different sites suggests that an extended empirical orthogonal function analysis would further enhance the patterns of variability. Unfortunately, some of the time series are too short and too much data would be lost by this technique. Instead, we chose to calculate the EOFs of the time series lagged with respect to each other according to Figure 10a. This is done for the 15 longest lagged time series spanning a period of 39 years (corresponding to 1950-1988 at OWS Charlie). S and stations northeast of Iceland which were not well correlated with the others are not included in the EOF analysis. The results are presented on Figure 11. The regression of the individual time series on the PCs are also computed.

PC1 of the lagged salt content time series explains 70% of the variance (Figure 11a). The associated EOF has largest amplitude at stations along the slope around the Labrador Sea with generally less variance toward the northeast (Figure 11b). It explains more than 65% of the local variance at most sites (Figure 11c) with the

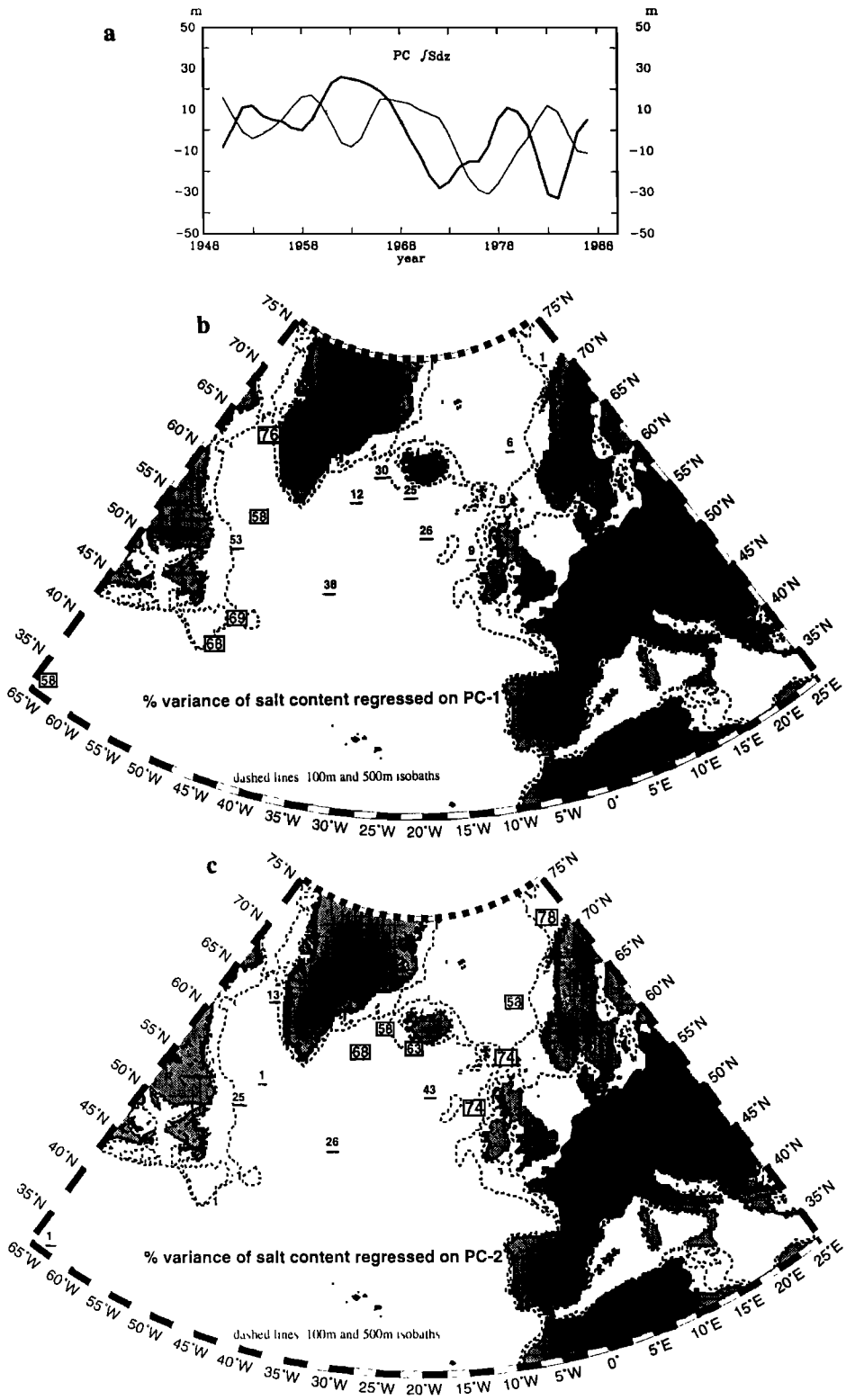

Figure 9. EOF decomposition of the salt content time series. (a) The time series of PC1 (heavy line) and PC2 (light line). Percentage of the variance regressed on (b) PC1 and (c) PC2 (see rms variability of salt content in Figure 7c). Large values are boxed with font size increasing with value. The spatial amplitude of the EOFs (not shown) is positive at all points.

exception of the central Labrador Sea time series where only 45% of the variance is captured by PC1. Not much of the temperature variance projects onto this mode, except off the Grand Banks and in the central subarctic gyre and Irminger Sea (Figure 11d). The weaker correlation between T and S time series at other sites is the main reason for the small share of temperature variance represented by this PC.

It is questionable whether this mode is characteristic of the whole record or only of the time of the GSA. Without the 15-year interval corresponding to the GSA, PC1 represents only 64% of

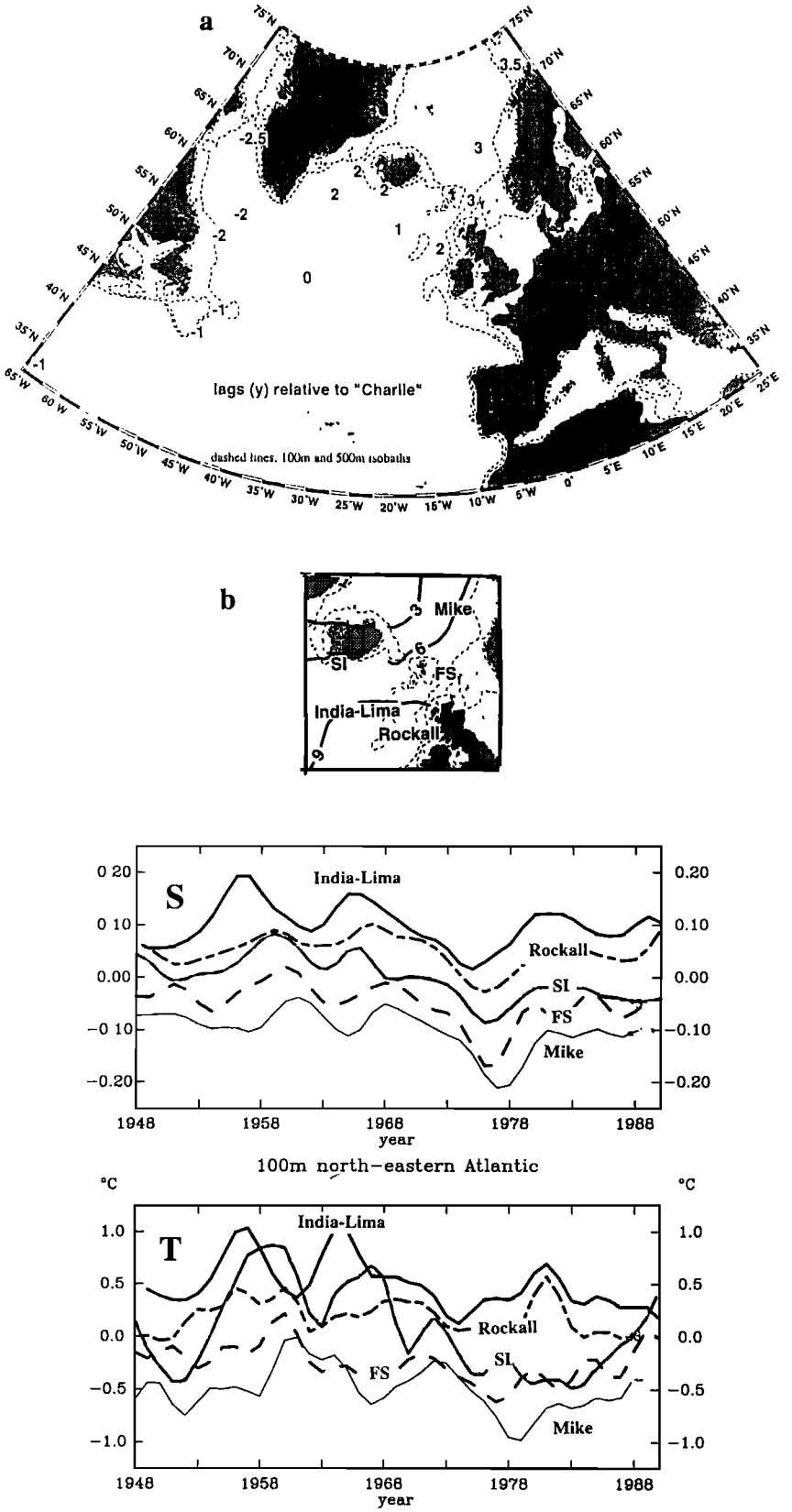

Figure 10. (a) Map of the lag (in years) relative to OWS Charlie which maximizes the correlation between salinity variability at each site and salinity variability at Charlie. (b) Northeastern Atlantic time series of temperature and salinity deviations. Each curve is offset by 0.25°C in temperature or 0.05 in salinity. From top to bottom, OWS India-Lima, Rockall, SI (Svelgobanki), FS (Faroe-Shetland Channel), and OWS Mike (a map indicating the location of these sites is plotted in the top panel of the figure with the 100- and 500-m isobaths).

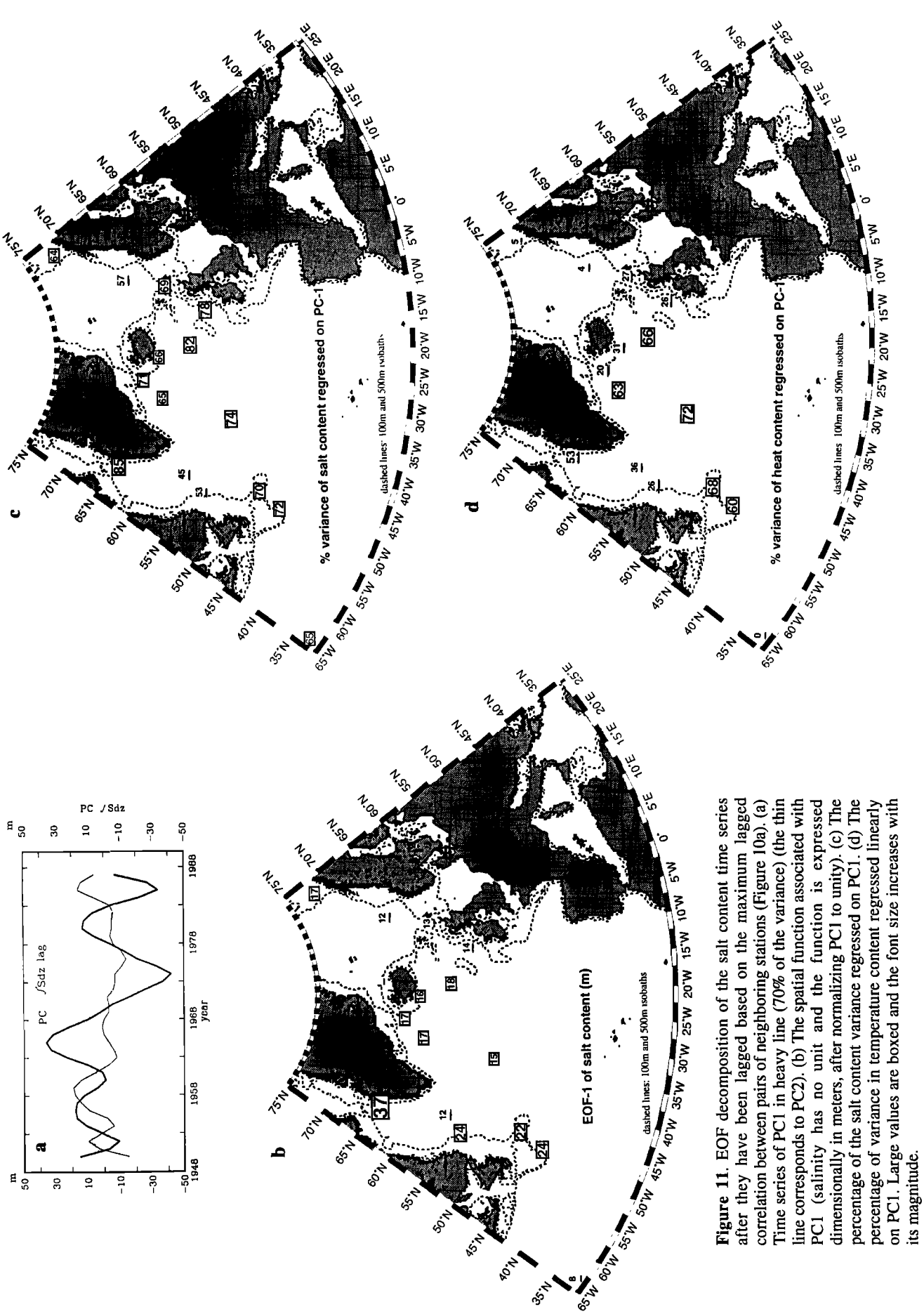

Figure 11. EOF decomposition of the salt content time series after they have been lagged based on the maximum lagged correlation between pairs of neighboring stations (Figure 10a). (a) Time series of PC1 in heavy line (70% of the variance) (the thin line corresponds to PC2). (b) The spatial function associated with PC1 (salinity has no unit and the function is expressed dimensionally in meters, after normalizing PC1 to unity). (c) The percentage of the salt content variance regressed on PC1. (d) The percentage of variance in temperature content regressed linearly on PC1. Large values are boxed and the font size increases with its magnitude.

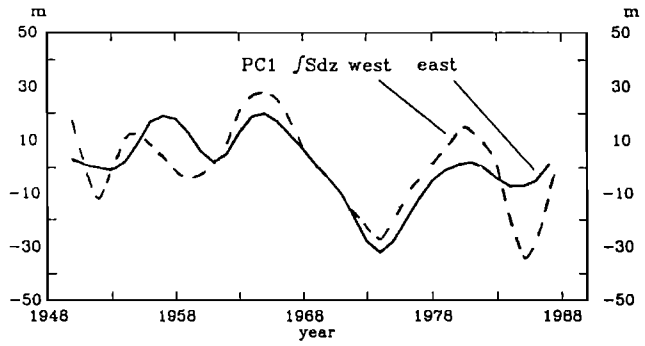

Figure 12. Time series corresponding to the first mode in the EOF decomposition of eastern and western salt content series (east and west, respectively, of Charlie; lags corresponding to Figure 10a applied).

the total variance, and the corresponding pattern mode is more weighted toward the western time series. This is also illustrated when we performed a principal component decomposition separately for the eastern and western lagged salt content time series (Figure 12): the correlation between the western and eastern PC1 is only 0.74. The western first PC of salt content is quite similar to the first PC for the upper ocean salinity at all stations (lagged or not lagged, not shown), which is not surprising considering that the time series of salinity in the slope water of the northwest Atlantic have the largest variance.

We will now briefly describe the EOFs of temperature and vertically integrated temperature. The temperature time series analyzed here are more noisy and less correlated to one another than the salinity time series. Therefore the analysis of temperature is less robust than the one for salinity. Partly due to this, and partly to the different spatial domains investigated, we find significant differences between our results and the time series associated with the second EOF of winter surface temperature in DB. For vertically integrated temperature (or temperature), there is little evidence of propagation. Both with and without lags (Figure 13 corresponds to the decomposition without lag) the first PC of vertically integrated temperature contains approximately 50% of the variance. Adding a lag between the sites does not increase the percentage of variance explained by the first PC. The first PCs for temperature and vertically integrated temperature are highly correlated at a value of 0.88 (Figure 13a). They are closer to that of salinity when they are estimated from the lagged time series, albeit with more negative values in the 1980s (correlation coefficient of 0.89 between the first PCs for vertically integrated temperature and salinity). Around 1980, the PC associated with the temperature mode displays high values, as does the salinity PC, but the heat content mode has smaller values. The amplitude in the vertically integrated temperature mode (Figure 13b) is largest for the central North Atlantic sites, with a smaller amplitude in the northwestern and zero in the northeastern Atlantic. This contrasts with the first EOF of temperature (Figure 13c), which is weighted more toward the northwestern sites, because they have more variance. The first EOF of temperature presents a uniform sign across the subarctic gyre with amplitude decreasing from west to east. This pattern is consistent with DB EOF2 north of the Gulf Stream (note that their analysis does not include the western half of the subarctic gyre but does include the subtropical gyre).

The multidecadal variability of surface temperature depicted by *Kushnir* [1994] has a different temporal characteristics than the one depicted by the first PC of temperature presented on Figure 13a. *Kushnir* [1994] suggests that northern Atlantic surface temperature peaked around 1950, and *Schlesinger and Ramankutty* [1994] attribute a period of 76 years to this mode of variability. In the present data set, strong quasi-decadal variability restricts the ability to detect the multidecadal signal. We nonetheless attempt to delineate this variability by the differences between two 15 year intervals 1950/1964-1970/1984, as was done by *Kushnir* [1994]. For both the T and S fields at one particular depth (Figure 14), the difference maps exhibit small values along the slope around the Labrador Sea and in the eastern north Atlantic and European Seas and large values elsewhere. Particularly large values are found around Iceland, in the interior subarctic gyre and east of Newfoundland. At the slope current sites, the large quasi-decadal fluctuation renders the result sensitive to the particular year chosen to separate the two periods, and no conclusions can be drawn regarding the multidecadal variability.

5. Discussion

We presented evidence for the existence of large spatially coherent low-frequency fluctuations in the North Atlantic upper ocean salinity. Our results suggest that these salinity perturbations circulate around the subpolar gyre with a likely origin in the slope current area. This roughly corresponds to what is known of the large-scale circulation in this region [*Dietrich et al.*, 1980]. Therefore one possibility is that the propagation is caused by horizontal advection along the Polar Front and along the different branches of the North Atlantic Current (the signal reaches south Iceland earlier than the Faroe-Shetland Channel, which suggests a more direct propagation along the Reykjanes Ridge). However, the different sites correspond to very different water masses, with the sites in the northeast having water characteristics close to the ones of the North Atlantic Current, whereas the Labrador Current carries an Arctic water mass. Any mechanism proposed to explain this propagation should also explain why the temperature signal is more coherent with salinity in the west and less so in the east and why temperature presents less spatial contrast than salinity. Furthermore, the isopycnal analysis (section 3) suggests a different interpretation for the variability in the northeast than in the northwest. In the northeast, the T-S variability along the isopycnal surfaces is correlated with the surface variability. This contrasts with the variability along the continental slope in the northwest, where isopycnal displacements are correlated to the surface variability. We will first discuss qualitatively how the variability in various water masses can be connected by ocean processes, and then the possible effects of the atmosphere on temperature and salinity variability.

5.1. Ocean Processes

We have found that variability is largest in the cold and fresh near-surface water mass along the slope off the Labrador shelf and Grand Banks. The lack of interannual variability in these water mass characteristics is indicated by the T-S diagram (Figures 6a and 6b). It suggests that the two end-member water masses which form the subsurface water have not changed much in T-S space. The large vertical displacement of the isopycnals correlates well with the surface variability, implying changes in the amount of cold and fresh water input in this region. An interpretation which needs to be further supported is that there is

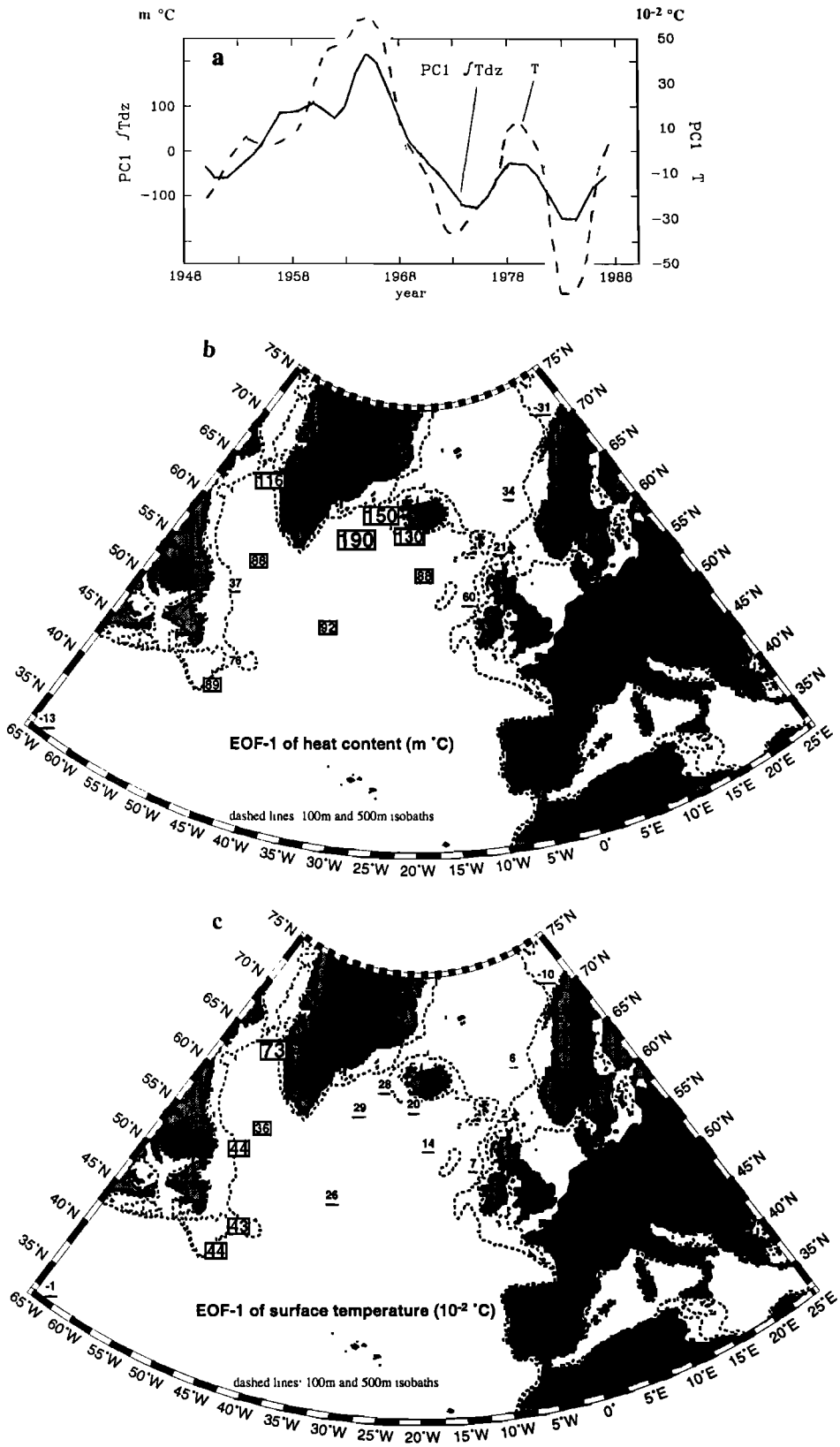

Figure 13. (a) The first time series for the EOF decomposition of temperature content and temperature (without lagging the stations). The spatial patterns for the first PC of (b) temperature content and (c) temperature. Large values are boxed and the font size increases with its magnitude.

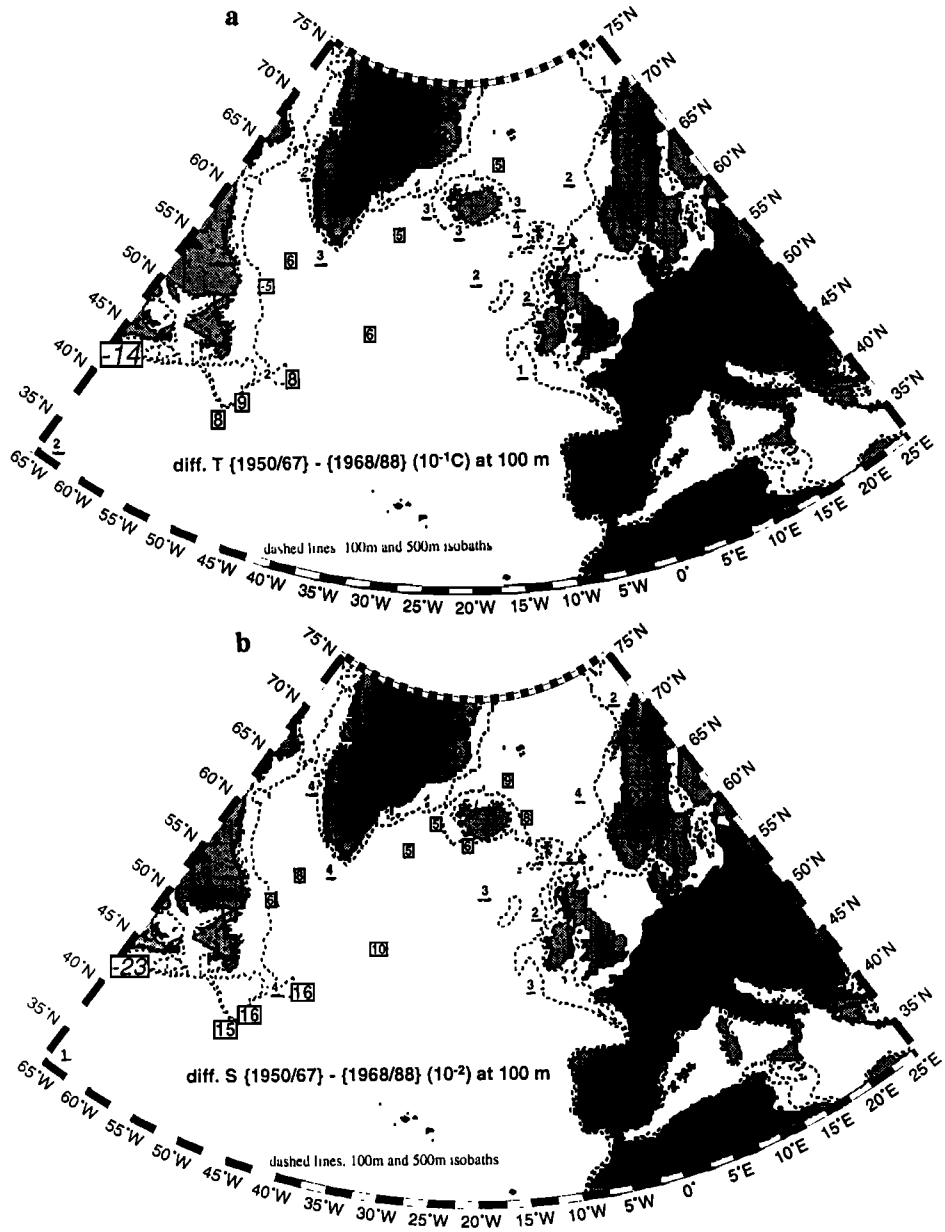

Figure 14. Difference between the first and second parts of the record (1967 is the middle year between the two periods compared of *Kushnir* [1994]). Maps are plotted both for (a) temperature and (b) salinity (on Figure 14a, notice some negative numbers off North America and Greenland). Large values are boxed and the font size increases with its magnitude.

a variability in the outflow of Arctic water penetrating in the subarctic through Greenland Strait or Davis Strait.

Winter ice cover is an important indicator of cold surface water. It is interesting therefore to examine the relationship between ice cover and surface salinity. We use ice concentration data from *Walsh and Chapman* [1990]. Spatially integrated sea ice concentrations are calculated in winter and early spring over Davis Strait and over the northern Labrador Sea and shelf. These regions show a correlation coefficient of -0.90 with PC1 of North Atlantic salt content with a 2-year lead, that is, with high ice concentration leading low salinity (Figure 15a). This 2-year lead is consistent with the lead of the salinity signal in the northern Labrador Sea with respect to the salinity signal in the central North Atlantic. Thus ice and salinity fluctuation are exactly out of phase in the Labrador Sea. A similar lag of northwestern Atlantic temperature relative to Davis Strait sea ice is presented in DB. Although sea ice cover north and south of 55°N in the western Labrador Sea is correlated (0.87 correlation coefficient at lag 1 year), there are marked differences between the two time series (Figure 15b): for instance, there is a large ice cover in 1983-1984 in the northern part, followed 1 year later by a maximum ice cover in the southern part. However, the previous ice cover maximum in 1972 happened in the southern part within 6 months of the maximum in the northern part. There is a clear minimum in ice cover north of 55°N in 1963, whereas the minimum south of 55°N is broad and centered on 1967. The 1969 peak in ice cover found north of 55°N is not found further south. Differences are also noted when comparing salinity and temperature time

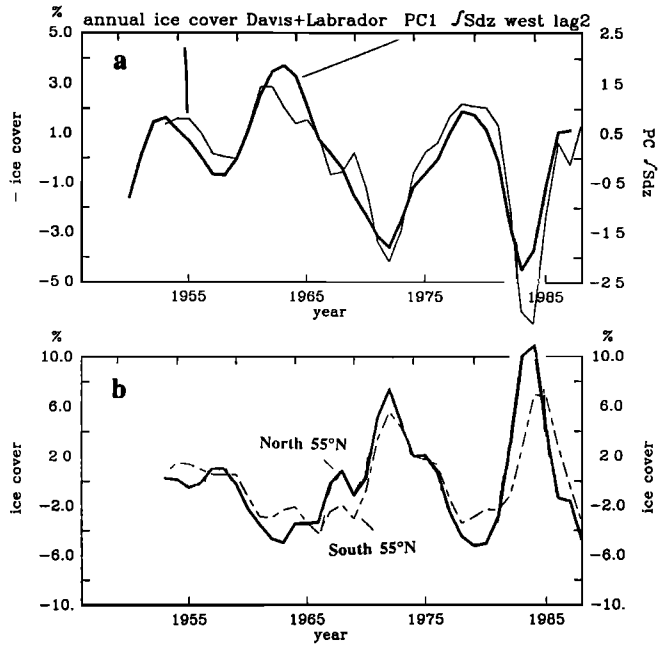

Figure 15. Spatially averaged ice concentration in various parts of the Labrador Sea. (a) Annual average of Labrador Sea-Davis Strait ice concentration (scale inverted) with the PC1 of salt content for the western Atlantic at the lead corresponding to the correlated signal in the slope current. (b) Winter ice concentration for the northern and southern Labrador Sea (north and south of 55°N).

series from the continental slope near Fylla Bank and Hamilton Bank, with the Flemish Pass 47°N, 47°W and with the time series at station 27 near Newfoundland (47°30'N, 52°35'W). In these areas, extensive winter sea ice is closely associated with the presence of a particularly cold and fresh water mass in the slope current (this relationship still holds when extending to 1995 time series of sea ice and salinity at 47°N, 47°W; C. Deser, personal communication, 1996). High sea ice cover is locally correlated with the low salinity, either because the low salinity is directly associated with cold water flowing in the east Greenland Current (or the Canadian Arctic and Baffin Bay) or that low salinity contributes to the near surface stratification and therefore winter surface cooling and ice formation [*Houghton*, 1996]. In either case, we can search for the origin of the signal in the variability of the outflow of cold Arctic water.

It is not possible to estimate the outflow variability with available data. By investigating changes in sea surface slope induced by steric effects in the upper water column, one can have some idea of the variability in the Labrador slope current located further downstream. The best sampled section is at 47°N. Offshore of the current, interannual variability in T and S is aligned along isopycnals, so there is little density changes at given depth and little steric change. On the shelf side of the slope current, however, interannual density anomalies contribute to more than 4 cm peak-to-peak interannual steric change from a depth of 400 m to the surface. In-phase changes of steric contribution to sea level are also found at station 27 on the shelf (47°30'N, 52°35'W) [*Myers et al.*, 1988, 1990; *Petrie et al.*, 1991] (the shelf time series differ a little from the Flemish Pass ones with peaks or troughs shifted typically by 1 year). This implies a peak-to-peak steric variability of the sea level slope across the slope current of the order of 4 dyn. cm (with a fairly shallow reference level at 400 m) compared to the 10-cm seasonal variability of the height difference across the Labrador Current [*Lazier and Wright*, 1993]. The interannual variability of steric heigh contributes to a large interannual variability in the baroclinic component of the slope Labrador Current. Although it is possible that the barotropic component of the current experiences some variability (as suggested by a diagnostic study of Reynaud [1994]), the slope current is strongly surface intensified [*Lazier and Wright*, 1993], so that the baroclinic component is likely to be a major contribution to the current variability near the surface. It is therefore expected that the near-surface slope current is stronger than normal when surface water is cold and fresh and weaker than normal when it is warm and salty. A similar argument is used by *Petrie and Drinkwater* [1993] to show that the transport along the Grand Banks at 43°N has decreased after 1968 or 1972. This suggests to Petrie and Drinkwater that after those years, most of the slope current is advected offshore north of 43°N.

It is thus likely that the signal in the slope current is related to large fluctuations of the slope current speed associated with changes in the outflow of fresh water from the Arctic. The slope current flows past Flemish Pass along the Grand Bank, and its waters spread into the interior where it mixes with warmer, saltier North Atlantic Current water. The time series of temperature and salinity at depth farther east (for example, east of the Flemish Cap) are strongly correlated with the vertical isopycnal displacements in the slope current at 47°N, 47°W. However, offshore, there is little variability in the subsurface density profile, and interannual T and S variability at a given depth is aligned along isopycnals on a T-S diagram, in marked contrast with the situation in the slope current. Thus the subsurface water mass which results from isopycnal mixing with the North Atlantic Current water is strongly influenced by the changes in the slope current transport (less water carried in the slope current results in a more salty and warmer interior on isopycnal surfaces). This mechanism of spreading of the anomalies through horizontal mixing between the slope current and the interior is different from that envisioned by *Dickson et al.* [1988], who did not consider changes in the intensity of the slope current. Our hypothesis does not explain the variability in the flow of Arctic surface water, as seen later when we discuss the atmospheric circulation effects in section 5b.

One could envision other scenarios which would result in simultaneous changes in the slope current and in the oceanic circulation in the interior. The observed ratio of T and S variability is comparable to the horizontal gradient of winter surface properties. This could be interpreted to imply that the T and S signals result from displacements of the currents. Such displacement of the Subarctic Front was suggested earlier by *Dooley et al.* [1984] to explain variability in the northeastern Atlantic. Surveys of the Subarctic Front south of Charlie suggest that the front experiences large coherent displacements [*Belkin and Levitus*, 1996]. However, in the past, some of the largest changes in upper ocean hydrography were not related to shifts in the position of the North Atlantic current (see R.R. Dickson et al., An investigation of the earlier Great Salinity Anomaly of 1910-14 in waters west of the British Isles, unpublished manuscript, 1987) discussion of the changes between 1910, a cold and fresh period, and the 1960s, a warm and salty period). Furthermore, changes in the interior circulation would not easily explain the lag observed from southwest to northeast in the interior of the subarctic gyre. Therefore this is a less likely explanation for the large scale salinity signal.

Fluctuations in the flow of fresh water to the subarctic gyre interior induce T and S variability north of the Subarctic Front. These could spread to areas where the Labrador Current water is strongly diluted with subtropical water, such as farther east at "Charlie" (Figure 6c) and even more so in the Rockall Trough and in the Faroe-Shetland Channel. One can diagnose from the salinity changes the change in heat content resulting from the change in advection of the cold water from the slope current. Adopting heat content values from the regression on the salinity PC1 for the western stations, one estimates peak-to-peak heat content changes between 1965 (+) and 1974 (-) of -300 m °C, associated with the GSA. This is equivalent to an average heat loss of 4 W m^{-2} over the 9-year period corresponding to the salinity decrease. In the northeastern Atlantic, this would induce a temperature signal of peak amplitude smaller than 0.5°C when distributed over the deep layer where the upper ocean signal is discernible (H). If there is divergence of the flow or horizontal diffusion of the signal, as suggested by the weaker salt content signals in the northeastern Atlantic, the temperature signal would be even smaller. Such an advected temperature signal would correspond to a 0.3 to 0.5 fraction of the observed temperature rms variability in the northeastern Atlantic.

The northeastern Atlantic water results from a large mixing of this cold water with warmer, saltier water advected by the North Atlantic Current from the subtropics. What effect would variability in the subtropical water mass have on temperature and salinity in this mixing-advection model? The small upper layer variability at S (Figures 7b and 7c) suggests that salinity variability in the warm water mass of the North Atlantic Current is smaller than in the Labrador slope current. However, in the northeastern Atlantic, the subtropical water contributes a larger proportion to the water mass than the Labrador slope water, so that the subtropical salinity signal can influence the time series in the northeastern Atlantic, although less so than would be the case for temperature. The correlation at 0 lag between the S and the Flemish Pass series is 0.73 for salinity, with no correlation in temperature. Remembering that T and S are correlated at Flemish Pass but not at S (Figure 8a), mixing advection between subarctic and subtropical water would result in the observed correlation in S (but not in T) between these sites and the northeastern Atlantic. However, it was not possible to reconstruct both the northeastern Atlantic temperature and salinity records from these two contributions with a simple advection-diffusion model (not shown). This suggests that direct air-sea forcing plays a significant role in modifying the low-frequency temperature variability. In the following section, we will examine qualitatively some aspects of this forcing and its impact on the variability.

5.2. Atmospheric Forcing

Wind variability operates either by modifying the oceanic circulation, inducing changes in the cross-frontal transports and eddy variability, or by the wind stirring of the upper layer. Heat and freshwater exchanges at the air-sea interface have direct impact on oceanic T and S but can also result in a change of circulation or vertical mixing. Some of these processes have been discussed in studies which are relevant for the North Atlantic region in question. *Ikeda* [1985] demonstrates that the wind variability would induce large seasonal variability in the transport of surface fresh water across the Labrador slope, either as fresh water or as ice. *Leach* [1990] comments on the relation between the wind and the Ekman transport of fresh water from the slope and shelf to the North Atlantic Current. It is also likely that part

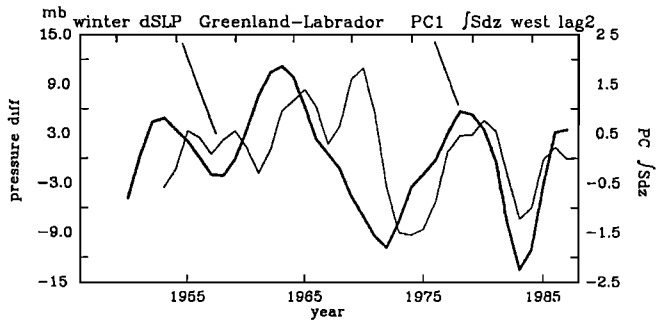

Figure 16. Time series of low-passed winter sea level pressure (SLP) (a 1-2-1 filter is applied for successive winters). The sea level pressure difference between Greenland and Labrador is overlaid with the PC1 of salt content for the western stations (presented for the maximum correlation at a 2-year lag which corresponds to the phase of the salinity signal near Labrador). The correlation coefficient between the two is 0.63.

of the hydrographic changes between the late 1950s and the early 1970s presented by *Levitus* [1989b], which have resulted in changes in the large-scale ocean circulation according to *Greatbatch et al.* [1991], were forced by the atmosphere. *Smith and Dobson* [1984] and *Lazier* [1973] discuss the effect of the heat exchanges and wind stirring on sea surface temperature variability at Bravo. *Cayan* [1992b] shows how the North Atlantic sea surface temperature responds to the heat fluxes on seasonal timescales. *Alexander and Deser* [1995] also show how the near-surface temperature at Charlie is controlled by the heat fluxes. *Cayan* [1992a] shows how the heat flux and evaporation patterns are related to the basin scale pressure field. D. Cayan and G. Reverdin (Monthly precipitation and evaporation variability estimated over the North Atlantic and North Pacific, unpublished manuscript, 1994) suggest patterns of the precipitation variability are associated with those of sea level pressure. Note, however, that there is more uncertainty in the freshwater flux at the sea surface and therefore on the atmospheric forcing of salinity.

To assess the atmospheric influence on low-frequency variability of temperature and salinity in the subarctic gyre, we will examine whether there exists a coherent atmospheric pattern associated with the oceanic one described above. Daily sea level pressure fields are available from the gridded National Center for Environmental Prediction (NCEP) analyses. Figure 16 presents the pressure difference across the Labrador Sea (a useful index for the mean wind and wind stress in winter: negative values indicate a stronger northwesterly component). The time series has been smoothed by a 1-2-1 filter as was done to the ocean time series. The results portray a significant low-frequency variability. The link with the salinity variability in the slope current is not strong (correlation coefficient of 0.63). The link is indicated here by the first EOF for the western stations with lead of 2 years, corresponding to the phase of the signal in the Labrador Current. The maximum wind anomaly in 1973-1975 lags the first salinity minimum (1971-1972), but in 1983-1984, the wind anomaly is simultaneous with the salinity minimum. *Lazier* [1973] also showed that vertically integrated salinity in the central Labrador Sea decreased each year during 1967-1972, covering periods of very different wind index.

From the pressure fields, we estimate surface geostrophic winds and surface winds. For that purpose, we use the formula of *Larson* [1975] which consists of a reduction of intensity of the geostrophic winds and a counterclockwise rotation diminishing

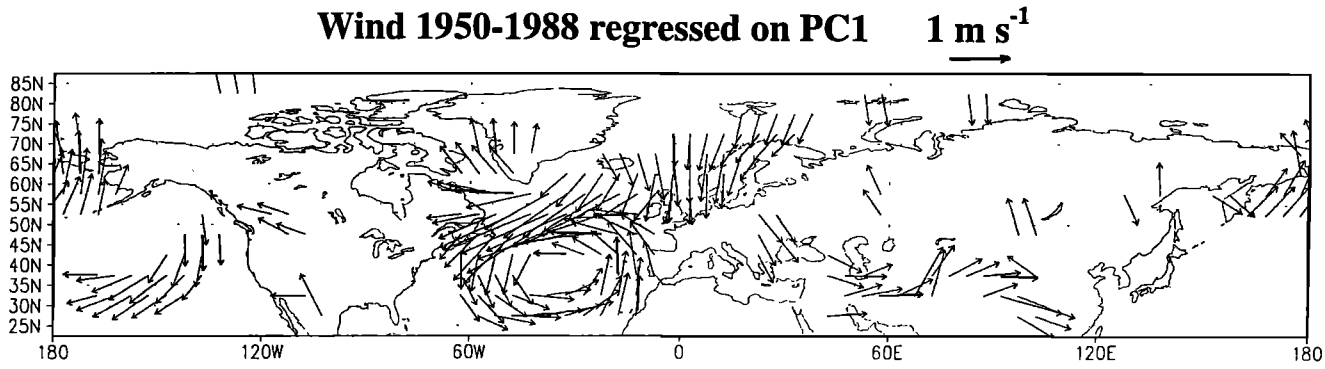

Figure 17. Surface wind calculated from the January-March National Center for Climate Prediction (NCEP) sea level pressure deviations from climatology regressed onto the PC1 time series for salt content. Only projections larger than 0.5 m s^{-1} are presented. The plotted vectors in the Atlantic are significantly nonzero at the 95% confidence level.

with increasing wind speed. Average monthly winds and wind stress are estimated from the surface daily winds. The Labrador Sea wind changes we discussed above appear to be part of a large-scale signal. DB showed how the same wind system is correlated with the surface temperature off the Grand Banks. When we regress the surface wind with the first salinity (or salt content) PC, we find an anomalous wind distribution pattern (Figure 17) reminiscent of the one corresponding to temperature of DB. In the central North Atlantic, the pattern is significant (at 95% confidence level) when the wind field leads PC1 by 1 year (not shown) or zero lag (Figure 17). Note that the phase of PC1 is with reference to the central Atlantic and a lead of 1 year corresponds to the phase of the salinity signal in the western Atlantic. The pattern during a salty (warm) interval displays weaker westerlies near 45° -60°N and stronger westerlies at 25° - 40°N, forming an anticyclonic anomaly around Greenland and a cyclonic curvature around the Azores, a pattern reminiscent of the NAO. This pattern is usually summarized in terms of the time series of pressure difference between Iceland and the Azores [*Bjerknes*, 1964]. The latter shows some agreement with the SST or salt content PC1 (Figure 18). The most conspicuous differences are in 1983 and for 1969-1970, when a positive pressure difference (weak westerlies) is associated with a period of cooling (freshening). The temperature time series are better correlated with the circulation index than the salinity time series (0.83 versus 0.71, respectively) with no clear indication that a lag or lead would improve the correlation.

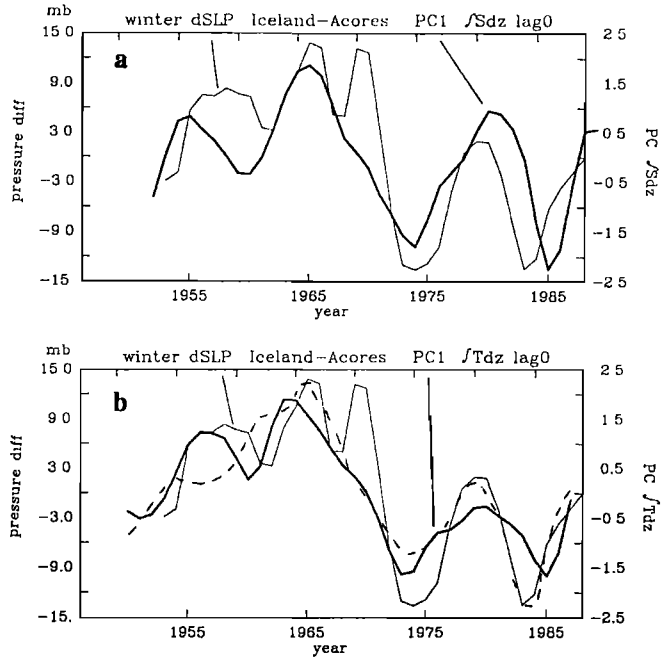

Figure 18. Winter sea level pressure difference between Iceland and Acores from NMC analyses (a NAO index with a 1-2-1 filter is applied for successive winters) overlaid on (a) the PC1 of salt content and (b) the PC1 of temperature content (solid line) and upper layer temperature (dashed line).

6. Conclusions

Several North Atlantic sites that have records of 3 or more decades of quasi-regularly observed hydrography, including salinity, were studied. When assembled, these records reveal a picture of upper ocean water mass modification and advection that is not discernible from temperature data alone. Salinity anomalies on multiyear timescales are quite coherent across the subarctic, more so than temperature. These fluctuations are strongest near the surface and decay with depth. In the northwestern Atlantic, the signal is within water which has a component originating from the Arctic and the slope currents of the Labrador Sea. In most other areas, the fluctuations penetrate the thermocline below the base of the winter mixed layer. This signal appears to be most energetic at periods of 10 years or longer. In the northwestern Atlantic, temperature fluctuations are well correlated with salinity fluctuations, alternating between cool, fresh states and warm, more salty ones. Furthermore, salinity variability is strongly correlated with ice extent in the Labrador Sea. Below the surface, the variability is caused mainly by displacements of isopycnals, and the analysis of *T-S* scatter diagrams indicates little change in water mass characteristics. We propose that salinity variability in the near-surface northwestern Atlantic is related to variations in the outflow of fresh, cold water. Periods with more of the fresh, cold water are associated with a more intense upper slope current and vice versa.

Within the subarctic gyre, we observe a propagation of the quasi-decadal salinity signal from station Charlie northward to the west of Iceland and northeastward to Norway. There, the signal is distributed over a thicker layer, so that the salinity signal is smaller. Spatial coherence between the northwestern and

northeastern Atlantic is higher for salinity than for temperature. In the northeastern Atlantic, the temperature and salinity are not as well correlated. One can explain this by taking into account the changes in the subtropical water mass component of the North Atlantic Current. The salinity at S in the subtropical gyre is correlated with the one in the northwestern Atlantic, but the temperature is not. Advection and mixing of subtropical water with Labrador Current water flowing to the northeast could therefore partially remove the correlation between T and S found in the Labrador Current. Our interpretation supports the *Dickson et al.* [1988] analysis of the Great Salinity Anomaly, an event that represents more than 50% of the variance in the 40-year-long records.

There is evidence that basin scale atmospheric circulation fluctuations produce wind anomalies that occur simultaneously with changes in temperature in the northwestern Atlantic; for example, northwesterly winds over the western North Atlantic are associated with low sea surface temperatures and vice versa. Because the atmospheric circulation is large scale (Figure 17), it is no doubt associated with a large-scale variability of the heat and freshwater fluxes. The magnitude of these fluxes is expected to contribute more to the observed variability in temperature than in salinity. This disparity could cause significant changes in the relation between temperature and salinity across the Atlantic. However, freshwater fluxes are very uncertain and such an association requires further investigation. The variability of ice concentration data and its association with the atmospheric circulation suggests that large variations in the salinity signal in the northwestern Atlantic originate from the northern European Seas in the mid to late 1960s (not shown [see *Mysak et al.*, 1990]). However, a contribution from Baffin Bay is also likely, at least in 1983-1984 when strong northwesterly winds were blowing over the Labrador Sea and Davis Strait.

Because the low-frequency salinity fluctuations are spatially coherent, their monitoring could be made with time series from a few well-chosen sites. This paper mainly focused upon the horizontal propagation of the salinity signal. We did not address many important scientific questions which would require longer time series as well as numerical modeling studies. An important question is whether the ocean-atmosphere relationship on the quasi-decadal timescale results from a coupled interaction or is the ocean responding to the atmosphere? It is also not clear whether changes in convection play a role in this quasi-decadal mode and at lower frequencies. The vertical structure of variability in the central Labrador Sea was documented on multiyear timescales by *Lazier* [1980], who interpreted it as the result from intermittent deep convection. According to this study, the salinity, integrated vertically to 1500 m (the maximum depth of convection in the period 1964-1974), does not display a seasonal cycle, but rather a very low frequency change on which high frequency changes of smaller magnitude (at periods less than a year) are superposed. *Lazier* [1995] suggested that it is through convection (for intermediate waters) and mixing (for deep waters) that near-surface signals diffuse vertically. This results in large modification of the subsurface waters, possibly contributing to changes in the thermohaline circulation. Convection is probably responsible for the lack of close correlation between the near-surface variability in the central Labrador Sea and around the rim of the Labrador Sea. Due to lack of observations, we were not able to examine most of the current variability, but we have speculated that there were large interannual variations in the slope current around the Labrador Sea. We also know very little about the current variability in the interior of the North Atlantic. Realistic ocean modeling can strengthen our conclusions on the role of advection in spreading the variability around the gyre.

Appendix

We need to assess to what extent the time series used in this paper from seasonally binned data are representative of the low-frequency variability. This issue will be explored from a few sites for which time series resolving the seasonal cycle can be constructed. The effect of sampling characteristics and data accuracy will be discussed. We will then investigate the seasonality of the low-frequency signal in the upper ocean. Finally, we will present examples of the constructed time series illustrating that the low-frequency time series are close to the seasonally binned data.

A1. Sampling

At each site, we construct continuous time series, with sampling ranging from a few times per day to twice a month. This sampling does not always resolve energetic high frequencies, which will therefore be aliased. There is also some spatial variability, in particular at OWS Mike, as successive stations are often separated by more than 20 km. This introduces a smaller correlation in time than at a fixed point, where the variability associated with mesoscale eddies is typically correlated over more than 1 week. To reduce the resulting artificial high frequencies, at most sites, the data are binned in time intervals of 5 days. Thus no information is retained at periods less than 10 days (30 days for S where sampling was usually done twice a month; and 60 days for the time series of monthly averages in the Rockall Channel). The 5-day mean position is fairly stable. The exception is OWS India-Lima, where a few sudden changes occur because we have constructed this time series by mixing three sites with close water masses, after adjusting their respective seasonal cycles: (60°N, 20°W) during January 1948 to March 1950 and August 1953 to June1954, OWS India at (59°N, 19°W) during May 1948 to June 1975, and OWS Lima at (57°N, 20°40'W) since July 1975 (Figure A1). At this site, changes of more than 200 km produce a hiatus in the high frequencies and intermediate frequencies. This can contribute to a transfer of variance to the high-frequency end of the spectra. However, provided that the climatology at the different sites is carefully adjusted, the few comparisons of near-simultaneous data suggest that the resulting distortion of the spectra is small.

A more severe problem in the records is provided by occasional long interruptions in the sampling. The worst ones are for ocean station S in 1979, for OWS Mike in May-October 1983 for salinity (there are other gaps of 6 months or less at subsurface), and for OWS India-Lima from December 1986 to April 1988 at the surface (also February-June 1989 at subsurface; furthermore, regular subsurface sampling began later than at the surface: May 1961 at 300 m and deeper and only September 1963 in the upper 250 m). OWS Charlie has even more interruptions (the largest ones from January 1974 to August 1975, October 1980 tooFebruary 1981, July to December 1982, and December 1987 to December 1988). We retain OWS Charlie despite these large gaps, because studies of the more complete temperature time series [*Levitus et al.*, 1995] indicate a larger variance at the very low frequencies than at the intermediate range, which is most seriously affected by the gaps. Small gaps in the time series are bridged by a natural cubic spline. For the long interruptions (larger than 2 months), proxy data are introduced once a month

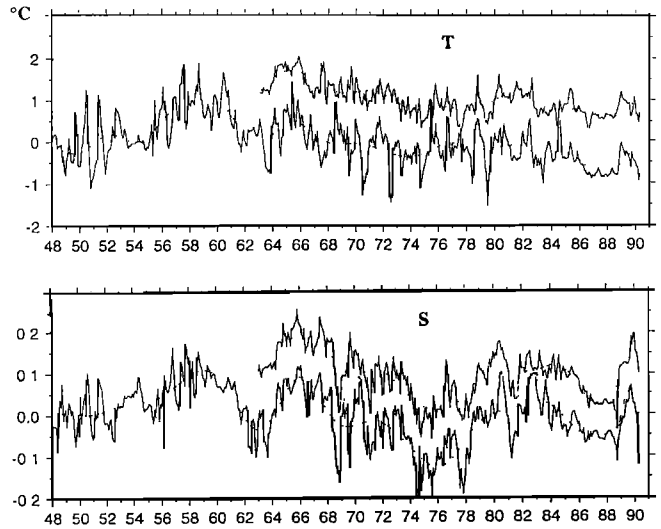

Figure A1. Time series of salinity and temperature deviations from the seasonal cycle at India-Lima. The time series constructed from 5-day averages have been Gaussian filtered with an e-folding response at 1 month. The dotted curves are the filtered curves with a cutoff at 3 years. On each plot, the bottom curve is at 0 m and the top one (shifted upward by 1∞C and 0.1 in salinity) is at 100 m (before 1963, sampling is less frequent at 100 m, so that we could not construct 5-day averaged data for that period).

from the linear interpolation between the end points (after removal of an estimated seasonal cycle). At OWS Charlie, this has an important effect on the spectral distribution of variance, although, based on simulations with other time series, it is expected that the variance in the very low frequencies is not strongly modified.

A2. Data Accuracy

We list here certain data problems which were tentatively corrected. Early salinity samples were titrated and errors sometimes resulted from using an incorrect reference or because the standard water had evolved or the samples had breathed before being analyzed. Errors are relatively easy to trace at OWS Mike, because of the associated sampling of the deep Norwegian Sea water, for which the evolution is small and well monitored [*Gammelsrød et al.*, 1992]. We assume that surface samples that were collected simultaneously with the hydrographic cast deep samples would present the same biases. The titration error for the United Kingdom samples from the Rockall Channel, OWS India-Lima, and the Faroe-Shetland sections before 1958 has been estimated from the Norwegian Sea deep water sampled in the Faroe-Shetland Channel, by comparing to the reference salinity profile in this water with the simultaneous Danish or Norwegian cruises. The titration error is particularly large in 1949 and early 1950 and evolves in time. As we do not know exactly when the samples of the OWS ships were analyzed, the correction applied is relatively uncertain at any given time. After 1958, the United Kingdom samples were titrated using an Autosal salinometer at Lowestoft, and we assume that the error on these measurements is less than 0.01.

There are additional errors in surface measurements [*Parker and Folland*, 1991; *Reverdin et al.*, 1994]. Temperature measured from a bucket or an intake presents a systematic bias and an unclean bucket can result in a too high salinity. Also, some surface samples might not have been carefully stored. We expect that the resulting errors in the Rockall Channel time series are relatively small (order of 0.01 psu) because of the careful checks being applied to the data. For the other sites, we compare the surface level and the first subsurface measurements (near 10-m depth) of hydrographic casts. At OWS Mike, the climatology shows a large density inversion at the surface [see *Gammelsrød et al.*, 1992], which results from a bias in the surface data of the Norwegian stations, in particular in 1977-1988, when it commonly exceeds 0.05 in salinity. The other sets of hydrographic casts present lesser systematic differences between the surface and subsurface level salinities, although there is also evidence for some systematic bias in the surface level data from Dutch or United Kingdom data since 1977. Unfortunately, we have few direct comparisons for United Kingdom data collected before 1967, and we will assume that 1967 comparisons apply to these earlier data. We will assume that these biases are also characteristic of the surface data collected from the weather ships during the same period. This assumption may be optimistic, as it seems that some of the surface data of the weather ships are not of the same quality as the surface level of hydrographic casts. For example, in late 1982 to early 1983, we find many dubious Dutch surface data at OWS Lima. Biases for surface temperature in cast data seem to be small, although quite systematic (of the order of 0.1°C) for parts of the records and are also corrected. Again, we

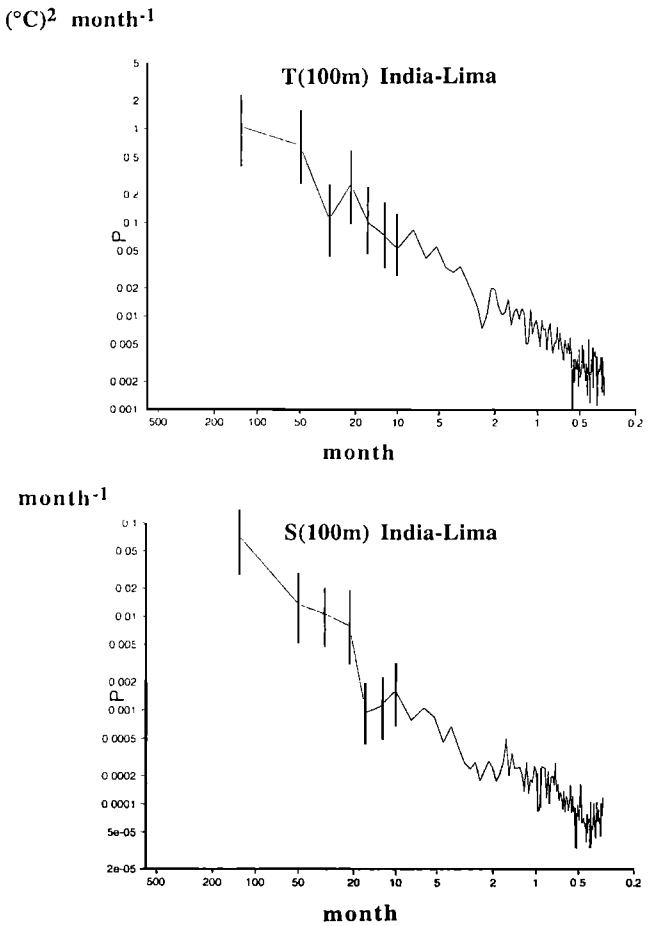

Figure A2. Power spectra of 100-m temperature and salinity at India-Lima from the 5-day averaged time series after removal of the seasonal cycle (90% uncertainty range of these band averaged spectra indicated at the lowest frequencies).

have no direct comparison for United Kingdom data before 1967. Other evidence [*Reverdin et al.*, 1994] suggests that these pre-1967 biases have been small, even in winter. This is supported by a comparison of the Comprehensive Ocean-Atmosphere Data Set (COADS) SST time series with our SST time series in the Rockall Channel, which exhibits an rms difference of 0.16°C at low frequencies (cutoff at a period of 3 years). It is at this site and in the Faroe-Shetland Channel that the differences between COADS SSTs and our SST time series are qualitatively the largest because the interannual SST signal is so small.

It is difficult to directly assess the effect of these errors on the time series. Part of the error is in biases which evolve over many years and can therefore affect the low frequencies analyzed. The hope is that the errors differ between sites and are therefore not captured in the EOF decomposition. The effect on the low frequencies of the white noise part of the error and of the aliasing due to the sampling can be estimated from the spectra at well-sampled sites. For example, a power spectrum is presented for OWS India-Lima (Figure A2) which is very red, so that the error effect for this time series is less than 1% of the signal variance at periods longer than 3 years for T and S.

A3. Seasonality of the Low-Frequency Signal

Because of insufficient sampling, we are often tempted to combine data from different seasons. This is only meaningful if different seasons provide statistically equivalent realizations of the same low-frequency signal. Clearly, the seasonal changes of upper ocean stratification and of the surface forcing could modulate the deviations from the average seasonal cycle. For example, at OWS Bravo in the Labrador Sea, or in the northwest Atlantic [*Bauer et al.*, 1991], a large near-surface summer freshening results from advection of stratified fresh water or sea ice mostly from the Labrador shelf. At that site, there is more year-to-year surface salinity variability during summer than during winter. However, even there, winter and summer anomalies are correlated. Whether data from different seasons should be considered together for assessing the low-frequency variability is also questionable in areas where different water masses are present in the different seasons, as in the upper ocean waters off the Fylla Bank [*Buch*, 1984] or for the Labrador shelf [*Lazier*, 1982]. However, sampling is not sufficient in those areas to conclude whether there are significant differences in interannual salinity deviations between the seasons. Indeed, off Fylla Bank, the differences between sampling in different seasons (April, July, November) are not sufficient to mask the large low-frequency signal [*Blindheim*, 1974; E. Buch and M. Stein, Temperature and salinity at the Fylla Bank section, west Greenland, unpublished manuscript, 1987].

The seasonal variations in interannual signal can also be investigated at the more densely sampled sites occupied by the weather ships and the ocean station S time series. At these sites the high-frequency fluctuations can be filtered before binning data in seasonal averages. Time series can be constructed retaining only the averages for a particular season. Below 25 m, they usually present a similar low-frequency signal during the different seasons. This is particularly true at OWS India-Lima, where low-frequency time series constructed from data of different seasons are almost indistinguishable from one another. For example at 100 m, the rms difference between S (T) time series from winter and summer data is 0.020 (0.18°C) compared to a rms interannual variability of 0.055 (0.35°C). This indicates not only that the interannual low-frequency variability has similar characteristics in the different seasons but also that the energy at the few months to few years timescales which is aliased with this sampling of a few months each year does not have a too strong effect at the low frequencies. This is confirmed by spectral analysis of 5-day binned data at that site which shows a red spectrum in this frequency range for S and T with a logarithmic slope of at least -1.5 for S. At 100 m, the variance between 3 and 30 months is 0.003 (0.056 $(°C)^2$) for S (T) compared with a variance at lower frequencies of 0.011 (0.055 $(°C)^2$). The spectral analysis also indicates that the ratio of low-frequency over high-frequency variances is larger for S than for T, a conclusion which holds for most of the time series we examined. For most time series, we bin the individual deviations from the seasonal cycle each year and then estimate the low-frequency cycle, so that the high frequencies can leak to the lower frequencies. From the preceding discussion, we expect that there is less aliasing of the variability at periods of a few months to a few years in the S low-frequency time series than in T. Note that the leakage at the 2-year period is removed by the 1-2-1 filter that we apply on the estimated low-frequency time series.

Whether these conclusions can be extended to the upper 25-m layer is not certain. When one considers only data from the cold season, the low-frequency surface signal is usually close to the subsurface one with differences which could result from aliasing of eddy variability. At OWS India-Lima (Figure A1), for example, the wintertime correlation coefficient between the surface record and the 100-m record is 0.84 (0.90) for S (T) (for these time series, a correlation coefficient of 0.7 is significantly nonzero at the 99% confidence level). The summer season correlation is less with correlation coefficient of 0.74 (0.28). In summer, it is typical that correlations between the surface and subsurface are smaller for temperature than for salinity. Although we find significant correlations between surface salinity anomalies from summer to winter at OWS India-Lima, Rockall and Charlie, they are less certain at two other sites, OWS Mike and ocean station S near Bermuda. It appears that the summer surface salinity deviations have less significance for monitoring the low-frequency hydrographic variability than those in winter or early spring. Similar conclusions were reached in the study of 100 years of surface and hydrographic data in the Faroe-Shetland Channel [*Reverdin et al.*, 1994].

If we assume from the above discussion that different seasons portray the same interannual variability as was found for subsurface levels, then the uncertainty from combining data from the different seasons is related to the relative amplitude of the error on the seasonal cycle compared to that of the low-frequency variability. The seasonal cycle of temperature is usually significant in the upper 200 m, but even at well-sampled sites it is rarely possible to estimate a significant seasonal cycle of salinity below 50 m, because of the high-frequency variability or data errors. We also find that the ratio of interannual to seasonal rms variability is smaller for T than for S. For example, at 50 m at OWS Charlie, this ratio is 0.4 for T compared to 2.0 for S, and at OWS Mike, it is 0.2 for T compared to 1.3 for S. These few sites suggest that the uncertainty on the estimated seasonal salinity cycle is not likely to be a serious problem for estimating the low-frequency signal below 50 m. However, the situation is probably less favorable close to shelves (see, for example, the large salinity seasonal cycle over the Labrador shelf of *Lazier* [1982]); therefore in the slope current sites around the Labrador Sea we only retain data from the regularly sampled seasons: April-November off Fylla Bank and May-November off Hamilton Bank.

At the sites where continuous time series cannot be created, data are binned into seasonal deviations, which are then fitted by

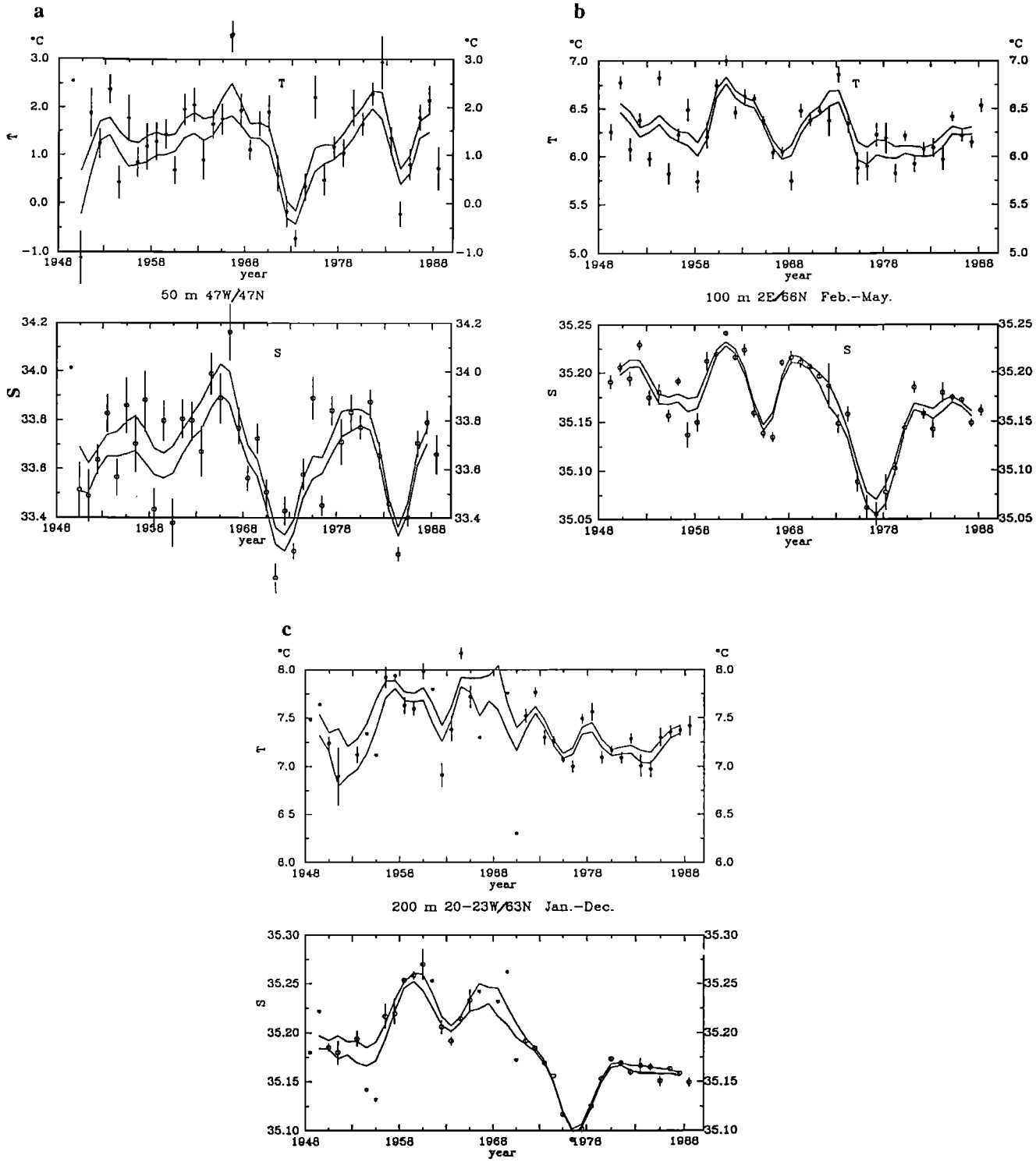

Figure A3. Seasonal averaged (top) temperature and (bottom) salinity (February-May at 66°N, 2°E and January-December at other sites) at (a) 50 m, (b) 100 m, and (c) 200 m.. Stars indicate when there are less than 3 data; dots indicate when there are more than three data. The ± s range of the low-frequency estimates is contained between the two curves.

a cubic spline. The resulting series is then smoothed by a 1-2-1 filter over successive yearly values. At the well-sampled sites, we have compared this processing to the more correct filtering based on the Fourier decomposition of the regularly sampled data and have found differences in variance between the two low-frequency curves of the order of 10%. This error is marginal compared to the uncertainties resulting from the sampling for the less well-sampled sites. Examples of the seasonally binned data are presented on Figure A3. These examples suggest that the low frequencies are a large part of the signal contained in the seasonally binned data (more so for Figures A3b and A3c than for Figure A3a in the Flemish Pass). This results in relatively low uncertainties on the low-frequency time series indicated by the ±s range plotted on Figure A3, assuming that the year-to-year variability is a "noise "on the low-frequency signal. We should also mention for OWS Alpha an additional error for the salinity

time series after 1974. Because there are too few salinity stations in the central Irminger Sea after 1974, we first create the temperature time series. Then we construct a proxy salinity time series from the temperature time series based on the correlation between temperature and salinity in the 1954-1974 station data. Finally, we correct this salinity time series using the few salinity data available.

Acknowledgments. We are grateful to the numerous oceanographers who have pursued long-term hydrographic investigations, without which studies of the ocean variability would not be possible, in particular in the United Kingdom, Denmark, Norway, and Iceland. We are particularly grateful to Harry Dooley at ICES for his help in complementing the hydrographic data distributed by NODC. Steve Peng and Dmitriy Pozdnyakov performed some of the analyses. Martin Visbek, Bob Houghton, Rosemary Morrow, and an anonymous reviewer provided a critical review of the manuscript. This study was partially funded by NOAA grant NA36GP0074 and by NOAA grant NA56GP0161. G.R. is also particularly thankful for the encouragement that late John Swallow has conveyed with enthusiasm throughout the years. This is Lamont-Doherty contribution 5589.

References

Aagaard, K., and E.C. Carmack, On the role of sea ice and other fresh water in the Arctic circulation, *J. Geophys. Res., 94*, 14,485-14,498, 1989.

Alexander, M.A., and C. Deser, A mechanism for the recurrence of winter time midlatitude SST anomalies, *J. Phys. Oceanogr., 25*, 122-137, 1995.

Bauer, J., H. Leach, and J.D. Woods, The seasonal variations of heat and fresh water contents between the Azores and Greenland, *Q. J. R. Meteorol. Soc.,117*, 1081-1104, 1991.

Belkin, I.M., and S. Levitus, Temporal variability of the subarctic Front near the Charlie-Gibbs Fracture Zone., *J. Geophys. Res., 101*, 28,317-28,324, 1996.

Bjerknes, J., Atlantic air-sea interaction, *Adv. Geophys., 10*, 1-82, 1964.

Blindheim, J., On the hydrographic fluctuations in the Labrador Sea during the years 1959-1969, *Fiskeridir. Skr. Ser. Havunders., 16*, 194-202, 1974.

Blindheim J., and H. Loeng, On the variability of Atlantic influence in the Norwegian and Barents Sea, *Fiskeridir. Skr. Ser. Havunders.,17*, 161-189, 1981.

Buch, E., Variations in temperature and salinity of West Greenland waters, 1970-1982, *Northwest Atl. Fish. Organ. Sci. Counc. Stud., 7*, 39-44, 1984.

Cayan, D., Latent and sensible heat flux anomalies over the northern oceans: Driving the sea surface temperature, *J. Phys. Oceanogr., 22*, 859-881, 1992a.

Cayan, D., Latent and sensible heat flux anomalies over the northern oceans: The connection to monthly atmospheric circulation, *J. Clim., 3*, 113-127, 1992b.

Deser, C., and M.L. Blackmon, Surface climate variations over the North Atlantic Ocean during winter: 1900-1989, *J. Clim., 6*, 1743-1753, 1993.

Dickson, R.R., and J. Blindheim, On the abnormal hydrographic conditions in the European Arctic during the 1970s, *Rapp. P.V. Réun. Cons. Int. Explor. Mer, 185*, 201-213, 1984.

Dickson, R.R., J. Meincke, S.-A. Malmberg, and A.J. Lee The "Great Salinity Anomaly" in the northern North Atlantic 1968-1982, *Prog. Oceanogr., 20*, 103-151, 1988.

Dickson, R.R., J. Lazier, J. Meincke, P. Rhines, and J. Swift, Long-term coordinated changes in the convective activity of the North Atlantic,*Prog. Oceanogr., 37*, 207-262, 1996.

Dietrich, G., W. Kalle, W. Krauss, and G. Siedler, *General Oceanography*, 2nd Ed., 626 pp., John Wiley, New York, 1980.

Dooley, H.D., J.H.A. Martin, and D.J. Ellett, Abnormal hydrographic conditions in the northeast Atlantic during the 1970s, *Rapp. P.V. Réun. Cons. Int. Explor. Mer, 185*, 179-187, 1984.

Ellett, D.J., Long-term water-mass changes to the west of Britain, *World Clim. Rep. WCP, 21*, pp. 245-254, World Clim. Program, Geneva, Switzerland, 1982.

Ellett, D.J., and N. MacDougall, Some monitoring results from west of Britain, *Tech. Ser. Int. Oceanogr. Comm., 24*, 21-25, 1983.

Frankignoul, C., Low frequency temperatures fluctuations off Bermuda, *J. Geophys. Res., 86*, 6522-6528, 1981.

Gammelsrød, T., and A. Holm, Variations of temperature and salinity at station M (66∞N, 2∞E) since 1948, *Rapp. P.V. Réun. Cons. Int. Explor. Mer, 185*, 188-200, 1984.

Gammelsrød, T., S. S. Østerhus, and Ø. Godøy, Decadal variations of ocean climate in the Norwegian Sea observed at ocean station "Mike"(66∞N, 2∞E), *ICES Mar. Sci. Symp., 195*, 68-75, 1992.

Greatbatch, R.J., A. Fanning, A.D. Goulding, and S. Levitus, A diagnosis of interpentadal changes in the North Atlantic, *J. Geophys. Res.,96*, 22,009-22,023, 1991.

Hansen, D.V., and H.F. Bezdek, On the nature of decadal anomalies in North Atlantic sea surface temperature, *J. Geophys. Res., 101*, 8749-8758, 1996.

Houghton, R., Subsurface quasi-decadal fluctuations in the north Atlantic, *J. Clim., 9*, 1363-1373, 1996.

Ikeda, M., Wind effects on a front over the continental shelf and slope, *J. Geophys. Res., 90*, 9108-9118, 1985.

Jenkins, W.J., On the climate of a subtropical ocean gyre: Decade timescale variations in water mass renewal in the Sargasso Sea, *J. Mar. Res., 40*, suppl., 265-290, 1982.

Jenkins, W.J., and J.C. Goldman, Seasonal oxygen cycling and primary production in the Sargasso Sea, *J. Mar. Res., 43*, 465-491, 1985.

Joyce, T.M., and P. Robbins, The long-term hydrographic record at Bermuda, *J. Clim., 9*, 3121-3131, 1996.

Keeley, J.R., Temperature and salinity anomalies along the Flemish Cap Section in the 1970s, *Northwest Atl. Fish. Organ. Sci. Counc. Stud., 5*, 87-94, 1982.

Kushnir, Y., Interdecadal variations in North Atlantic sea surface temperature and associated atmospheric conditions, *J. Clim., 7*, 141-157, 1994.

Larson, S.E., A 26-year time series of monthly mean winds over the ocean, 1, A statistical verification of computed surface winds over the North Pacific and North Atlantic, *Tech. Pap. 8-75*, Environ. Predict. Res. Facil., Nav. Postgrad. School, Monterey, Calif., 1975.

Lazier, J.R.N, The renewal of Labrador Sea water, *Deep Sea Res., 20*, 341-353, 1973.

Lazier, J.R.N., Oceanographic conditions at Ocean Weather Ship Bravo, 1964-1974, *Atmos. Ocean, 18*, 227-238, 1980.

Lazier, J.R.N., Seasonal variability of temperature and salinity in the Labrador Current, *J. Mar. Res., 40*, suppl., 341-356, 1982.

Lazier, J.R.N., The salinity decrease in the Labrador Sea over the past thirty years, in *Natural Climate Variability on Decade-to-Century Time Scales*, edited by D.G. Martinson et al., pp.295-304, Natl. Acad. of Sci., Washington, D.C., 1995.

Lazier, J.R.N., and D.G. Wright, Annual velocity variations in the Labrador Current, *J. Phys. Oceanogr., 23*, 659-678, 1993.

Leach, H., Interannual variability in the upper ocean in the North Atlantic, summer 1983 and 1986, *Deep Sea Res., Part A, 37*, 1169-1175, 1990.

Levitus, S., Interpentadal variability of salinity in the upper 150 m of the North Atlantic Ocean, 1970-1974 versus 1955-1959, *J. Geophys. Res., 94*, 9679-9685, 1989a.

Levitus, S., Interpentadal variability of temperature and salinity at intermediate depths of the North Atlantic Ocean, 1970-1974 versus 1955-1959, *J. Geophys. Res., 94*, 6091-6131, 1989b.

Levitus, S., J. Antonov, X. Zhou, H. Dooley, K. Selemenov, and V. Tsereschenkov, Observational evidence of decadal-scale variability of the North Atlantic Ocean, in *Natural Climate Variability on Decade-to-Century Time Scales*, edited by D.G. Martinson et al., pp. 318-326, Natl. Acad. of Sci., Washington, D.C., 1995.

Loeng, H., J. Blindheim, B. Ådlandsvik, and G. Ottersen, Climatic variability in the Norwegian and Barents Seas, *ICES Mar. Sci. Symp., 195*, 52-61, 1992.

Malmberg, S.-A., Hydrographic changes in the waters between Iceland and Jan Mayen during the last decade, *Jökull, 19*, 30-43, 1969.

Malmberg, S.-A., Hydrographic conditions in the East Icelandic Current and sea ice in North Icelandic waters, 1970-1980, *Rapp. P. V. Réun. Cons. Int. Explor. Mer, 185*, 170-178, 1984.

Malmberg, S.-A. and S.S. Kristmannsson, Hydrographic conditions in Icelandic waters, 1980-1989, *ICES Mar. Sci. Symp., 195*, 76-92, 1992.

Marsden, R.F., L.A. Mysak, and R.A. Myers, Evidence for stability enhancement of sea ice in the Greenland and Labrador Seas, *J. Geophys. Res., 96*, 4783-4789, 1991.

Mertz, G., S. Narayanan, and J. Helbig, The freshwater transport of the Labrador Current, *Atmos. Ocean, 31*, 281-295, 1993.

Myers, R.A., S.A. Akenhead, and K. Drinkwater The North Atlantic Oscillation and the ocean climate of the Newfoundland shelf, *NAFO SCR. Doc. 88/65 Ser.* N1508, 22 pp, Northwest Atl. Fish. Organ., 1988.

Myers, R.A., S.A. Akenhead, and K. Drinkwater, The influence of Hudson Bay runoff and ice-melt on the salinity of the inner Newfoundland shelf, *Atmos. Ocean, 28*, 241-256, 1990.

Mysak, L.A., D.K. Manak, and R.F. Marsden, Sea-ice anomalies observed in the Greenland and Labrador Seas during 1901-1984 and their relation to an interdecadal Arctic climate cycle, *Clim. Dyn., 5*, 111-133, 1990.

Palmer, T.N., and Z. Sun, A modelling and observational study of the relationship between sea surface temperature in the north-west Atlantic and the atmospheric general circulation, *Q. J. R. Meteorol. Soc., 111*, 947-975, 1985.

Parker, D.E., and C.K. Folland, Worldwide surface temperature trends since the mid-19th Century, in *Greenhouse-Gas-Induced Climatic Change: A Critical Appraisal of Simulations and Observations*, edited by M.E. Shlesinger, pp. 173-193, Elsevier Sci., New York, 1991.

Petrie, B., and K. Drinkwater, Temperature and salinity variability on the Scotian shelf and in the Gulf of Maine 1945-1990, *J. Geophys.Res., 98*, 20,079-20,089, 1993.

Petrie, B., J.W. Loder, J. Lazier, and S. Akenhead, Temperature and salinity variability on the eastern Newfoundland shelf: the residual field, *Atmos. Ocean, 30*, 120-139, 1991.

Reverdin, G., D. Cayan, H.D. Dooley, D.J. Ellett, S. Levitus, Y. du Penhoat, and A. Dessier, Surface salinity of the North Atlantic: Can we reconstruct its fluctuations over the last one hundred years?, *Prog. Oceanogr., 33*, 303-346, 1994.

Reynaud T.H., Dynamics of the Northwestern Atlantic Ocean: A diagnostic Study, Ph.D. Thesis, 267 pp., McGill Univ., Montreal, Quebec, Canada, 1994.

Schlesinger, M.E., and N. Ramankutty, An oscillation in the global climatic system of period 65-70 years, *Nature, 367*, 723-726, 1994.

Smed, J., Annual and seasonal variations in the salinity of the North Atlantic surface water, *Rapp. P. V. Reun. Cons. Int. Explor. Mer, 112*, 77-94, 1943.

Smith, S.D., and F.W. Dobson, The heat budget at Ocean Weather Station Bravo, *Atmos. Ocean, 22*, 1-22, 1984.

Talley, L.D., and M.E. Raymer, Eighteen degree water variability, *J. Mar. Res., 40*, suppl., 757-775, 1982.

Taylor, A.H., Fluctuations in the surface temperature and surface salinity of the north-east Atlantic at frequencies of one cycle per year and below, *J. Climatol., 3*, 253-269, 1983.

Taylor, A.H., and J.A. Stephens, Seasonal and year-to-year variations in surface salinity at the nine North-Atlantic Ocean Weather Stations, *Oceanol. Acta, 3*, 421-430, 1980.

Wallace, J.M., C. Smith, and Q. Jiang, Spatial patterns of atmospheric-ocean interaction in the northern winter, *J. Clim., 3*, 990-998, 1990.

Walsh, J.E., and W.L. Chapman, Arctic contribution to upper ocean variability in the North Atlantic, *J. Clim., 3*, 1462-1473, 1990.

Woodruff, S.D., R.J. Slutz, R.L. Jenne, and P.M. Steurer, A comprehensive ocean-atmosphere data set, *Bull. Am. Meteorol. Soc., 68*, 521-527, 1987.

D. Cayan, Scripps Institution of Oceanography, 9500 Gilman Drive, La Jolla, CA 92093.

Y. Kushnir, Lamont-Doherty Earth Observatory of Columbia University, Palisades, NY 10964.

G. Reverdin, Groupe de Recherche de Géodésie Spatiale, UMR CNES/CNRS 5566, 14 Avenue Edouard Belin, 31401 Toulouse, France (e-mail: reverdin@pontos.cst.cnes.fr)

(Received May 25, 1995; revised November 15, 1996; accepted November 19, 1996.)